Master Copy

CEBAF-PR-87-028

(e,e'N) REACTIONS

J. Mougey
Continuous Electron Beam Accelerator Facility
12070 Jefferson Avenue
Newport News, VA 23606

(e,e'N) Reactions

J. Mougey
Continuous Electron Beam Accelerator Facility
12070 Jefferson Avenue
Newport News, VA 23606, USA

Abstract

With the advent of a new generation of high energy, high duty cycle electron accelerators, a whole range of new nuclear and subnuclear phenomena can be investigated, in particular through coincidence experiments. This contribution focuses on one and two nucleon emission studies below pion threshold. After a brief review of recent experimental and theoretical work, the study of single nucleon densities through high energy (e,e'N) experiments is discussed. New insights in short-range multihadron phenomena are likely to be obtained through (e,e'p), (e,e'd) and (e,e'2N) reactions. Coincidence experiments, some of them involving polarization measurement, are described to study the free and bound nucleon electromagnetic responses.

I. Introduction

During the last three decades, a wealth of information on the structure of nuclei has been obtained from electro– and photoinduced reactions, confirming to a large extent the mean field description of nuclei. But, at the same time, electrons and photons have given the clearest indications for deviations from this "classical" picture, exhibiting the role of mesonic currents, nucleon resonances, relativistic effects and showing the need for introducing explicitly subnucleonic degrees of freedom. This is illustrated in Figure 1, showing recent results obtained in inclusive inelastic electron scattering on ^3He[1]. The observed spectrum cannot be quantitatively explained by simply adding the contributions from the two dominant single nucleon structures, i.e. the quasi elastic peak and the quasi-free excitation of the Δ_{33} resonance. Indeed, one can use this figure to point out different kinematical regimes where different processes can be enhanced:
– Near the top of the quasifree peak, single nucleon densities can be investigated efficiently. As the reaction occurs mainly on a single nucleon, this is also where bound nucleon electromagnetic properties can be studied.

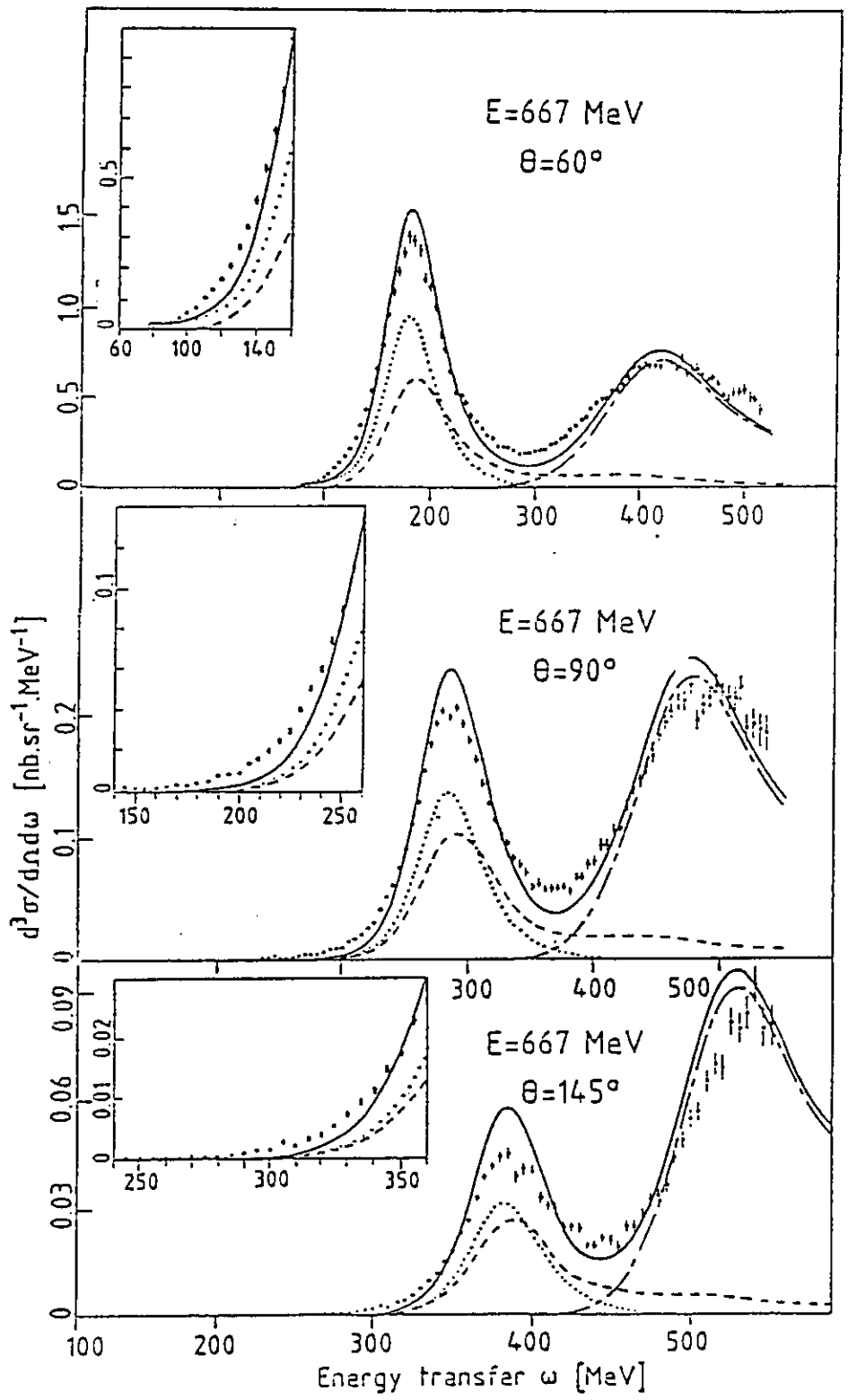

Figure 1 Cross sections for inclusive electron scattering off ^{3}He (data from ref. 1).

– On the low energy side of the peak, single nucleon contributions are limited to the high momentum tails of the density distributions. Two nucleon effects are expected, in particular around $x = 2$, where $x = Q^2/2M_N\omega$ is the Bjorken scaling variable. Here the two nucleons are emitted with low c.m. relative energy, possibly as a bound deuteron. Meson exchange currents are expected to contribute substantially. Quark clustering phenomena may be evidenced in this region [2].
– Two nucleon emission is assumed to be mainly responsible for filling in the "dip" between the quasi–free peak and the Δ – peak. Virtual Δ and N^* excitation with subsequent ΔN interaction is one possible mechanism. The two nucleons are emitted with a large c.m relative energy. It has been also suggested that four nucleon emission due to an intermediate $\Delta\Delta$ state may contribute substantially [3].

Of course, there is no clear cut between these different kinematical regimes, and the various processes are strongly interrelated.

II. Physics Around The Quasielastic Peak. Present Status And Issues

The separation of the transverse and longitudinal response functions in inclusive quasielastic electron scattering, performed recently on several nuclei from ^3He to ^{238}U[4–8] has clearly demonstrated that the interpretation of the quasielastic peak was not as simple as generally believed. The transverse response is found to agree qualitatively with proposed models, once pionic and short-range effects are taken into account. However, the longitudinal (Coulomb) response, which is simpler in nature because mesonic effects do not contribute in first order, tends to be significantly lower than theory. This is shown in figure 2 in terms of the "scaling functions" $F_L(y)$ and $F_T(y)$[9], which should be identical under the assumption of a quasifree nucleon knock out. A quantitative and fairly model independent way of summarizing these results is obtained by constructing the longitudinal sum rule which should approach the nuclear charge Z at high q. Figure 3 shows clearly a lack of strength reaching 40% at $A \sim 40$. Uncertainties in estimating the small (~10%) contributions from final state interactions (FSI) [10] cannot explain the discrepancy. Many other attempts have been made including introduction of correlations through RPA. More fundamental explanations have been given in terms of a modification of the e–p Coulomb coupling in nuclei, either through relativistic dynamics (σ –ω model) or quark models.

Two-nucleon effects, which have already substantial contributions at the quasielastic peak, (see figures 4 and 5) explain the major part of the cross section in the "dip" region. Two types of approaches have been used to get quantitative estimates: Laget [11] used a quasi–deuteron model to compute the meson exchange diagrams of figure 4a. Mulders [12] considers six–quark hadronic states to treat nucleon-nucleon correlations at short distances. The probability δ_6 of scattering off six quark clusters is adjusted to fit the transverse data, and found to be as large as 40% for ^{12}C around $\mid \vec{q} \mid = 500 MeV/c$. The results (figure 5) indicate a weak longitudinal and strong transverse contribution as short-range (pn) pairs dominate. Final states include NN, NΔ and $\Delta\Delta$ pairs.

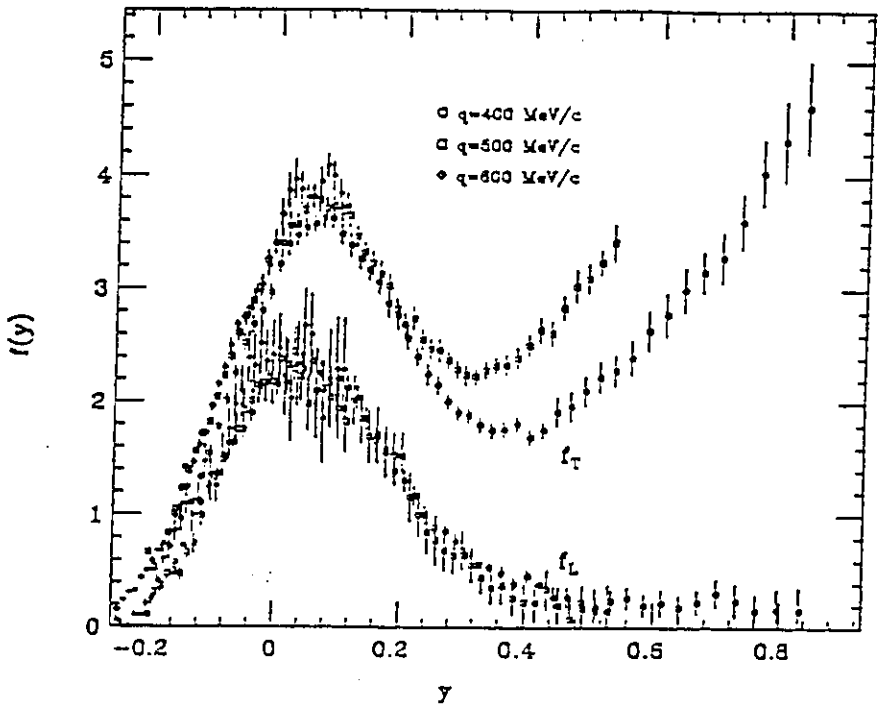

Figure 2 Reduced structure functions for $^{12}C(e,e')$ at quasielastic kinematics (from ref. 9).

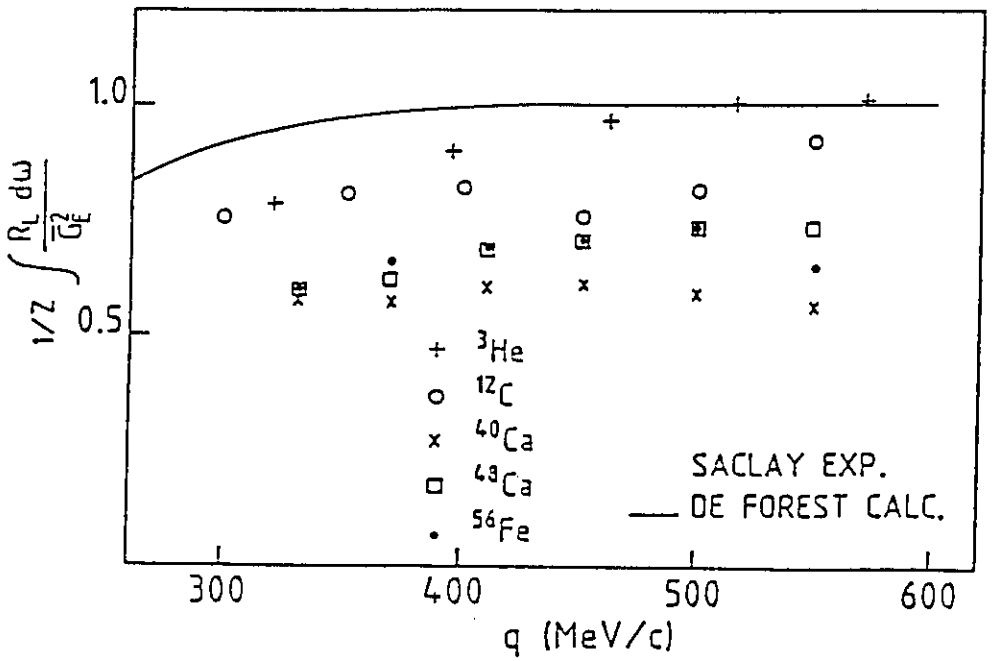

Figure 3 Longitudinal sum rule for different nuclei measured at Saclay ALS.

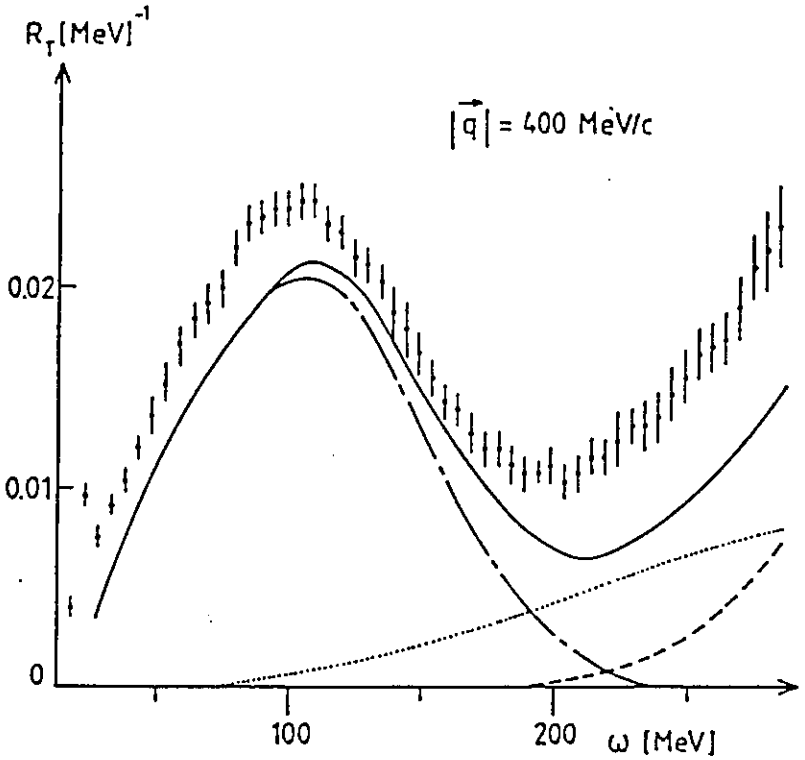

Figure 4 Transverse response function for ^{12}C at $|\vec{q}|$ = 400 MeV/c (from ref. 5). Curves, from Laget (ref. 11), show contributions from (–.–) one nucleon knock–out, (– – –) Δ – excitation, (.....) meson exchange currents, (——) total.

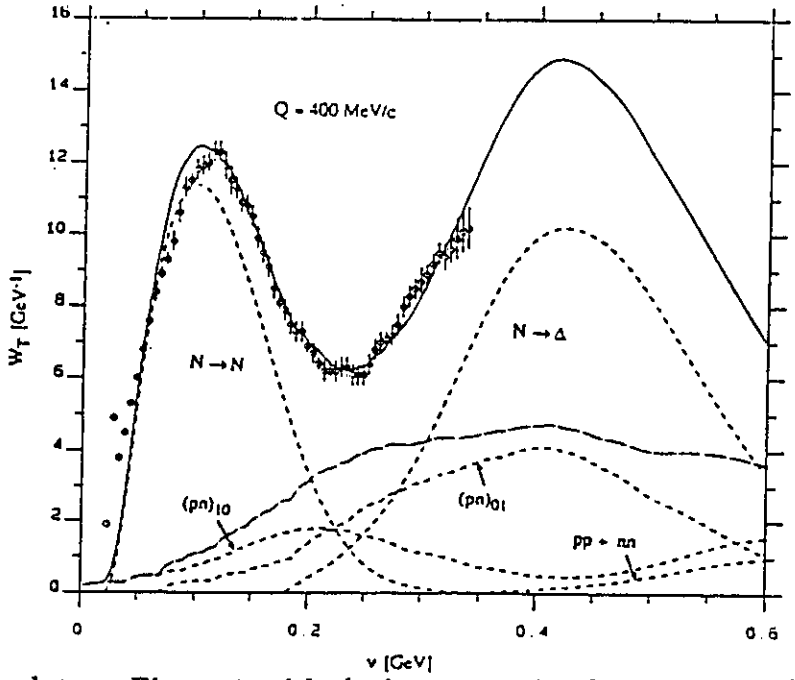

Figure 5 Same data as Figure 4, with the interpretation from Mulders (ref. 12) in terms of nucleons and 6- quark clusters.

Clearly, to go further, one must perform more exclusive experiments by detecting one or more emitted hadron in coincidence with the scattered electron, in order to single out specific channels. Although the relatively low duty cycle of the present electron accelerators makes such coincidence experiments difficult, (e,e'p) reactions have been studied in limited kinematical regions at several laboratories (Frascati, Saclay, Bates, Nikhef, ...) and the existing body of data allows to bring up some systematical trends. [13]

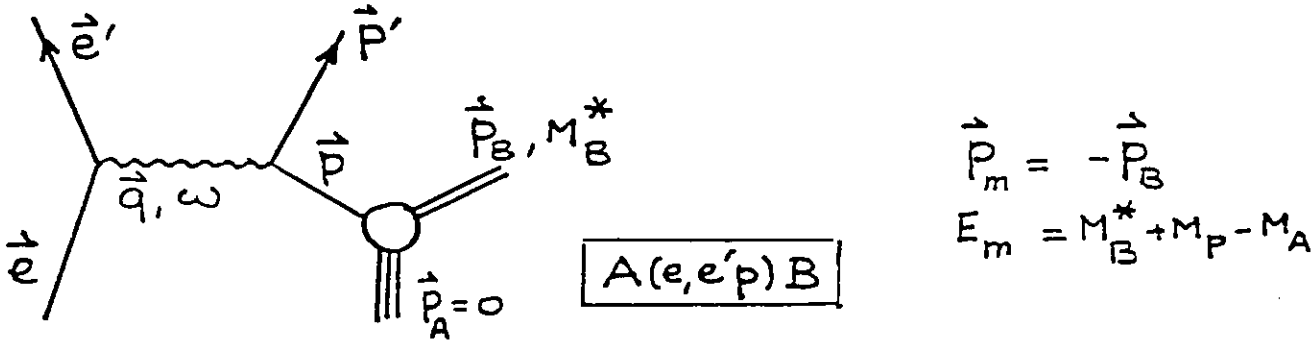

Figure 6 Direct nucleon knock-out process in the Plane Wave Impulse Approximation (PWIA)

The classical approach to analyze quasielastic (e,e'p) data is to assume that the virtual photon couples with a single (essentially free) nucleon current (see figure 6, introducing notations). Assuming further no final states interactions (PWIA) the cross section takes the usual form

$$d\sigma/d\vec{e}'d\vec{p}' = K\sigma_{ep}S(\vec{p}_m, E_m) \tag{1}$$

where K is a kinematical factor, σ_{ep} is essentially the free elastic electron–proton cross section and $S(\vec{p}_m, E_m)$, the spectral function, is the joint probability for removing a proton of momentum $\vec{p}_m$, leaving the residual system with an excitation energy E_m (relative to the target ground state). For the independent particle shell-model, one has

$$S(\vec{p}_m, E_m) = \sum_\alpha \mid \phi_\alpha(\vec{p}_m) \mid^2 \delta(E_m + E_\alpha) \tag{2}$$

where $\phi_\alpha(\vec{p}_m)$ is the momentum space wave function and the sum extend over all single particle quantum states α =(n,l,j). To a reasonable approximation, the factorized form of (1) can be generalized in the presence of final state interaction by replacing S by a "distorted spectral function" $S_D(\vec{p}', \vec{p}_B, E_m)$ depending on the particular choice of kinematics.

Within such a frame for analysis, nucleon momentum distributions have been obtained up to $\sim$ 600 MeV/c for ^2H,^3He,^4He and $\sim$300 MeV/c for A>4 nuclei. Occupation probabilities and separation energies have been extracted for a variety of nuclei. The high resolution of $\sim$ 100 keV in E_m which is routinely achieved at NIKHEF (see figure 7) demonstrates clearly the power of this experimental tool.

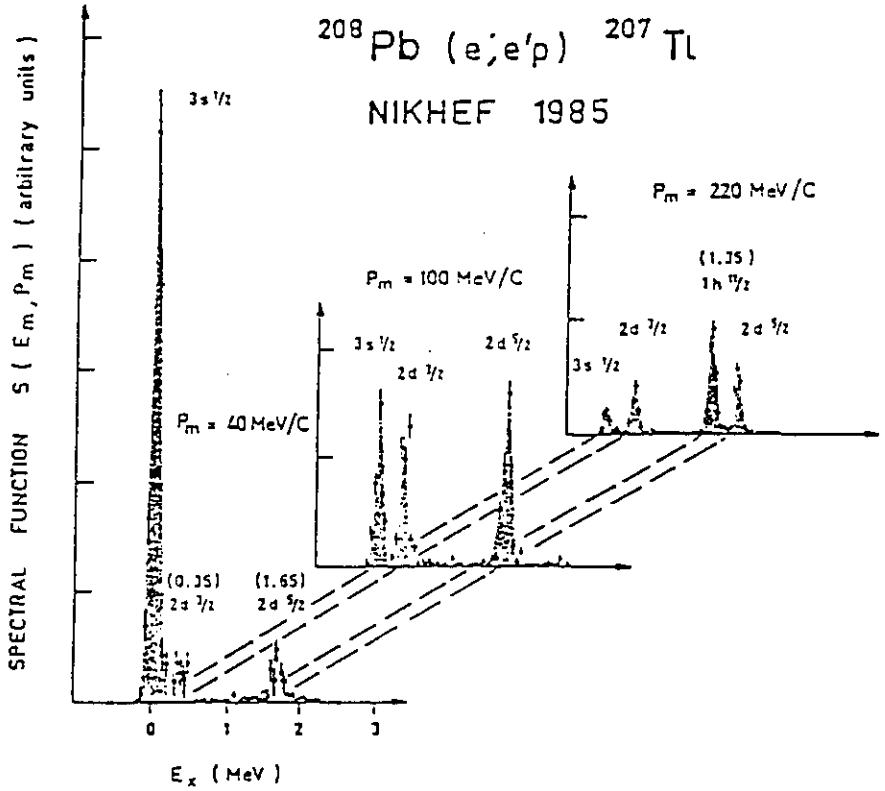

Figure 7 Spectral functions for the ^{208}Pb(e,e'p)^{207}Tl reaction at three different p_m–values (from ref. 56).

Although this simple description of the reaction has proven to be essentially valid (to within 20-50% over 3-4 order of magnitude) around the quasielastic peak, important systematic deviations have also been pointed out.

A lack of strength (up to 40%) in the spectroscopic sum rule

$$\int\int S(\vec{p}_m, E_m) d\vec{p}_m dE_m = Z \qquad (3)$$

has been observed when the integration is performed over the "shell model" region $p_m \lesssim$ 300 MeV/c, $E_m \lesssim$ 100 MeV (figure 8). An energy weighted sum rule [14] which relates the average separation and kinetic energies to the total binding energy per nucleon (proton) was shown also to fail consistently by $\sim$ 30% for A>4 nuclei, suggesting either a lack of one–body strength in the measured region, strong contributions from these body forces, or a breakdown of the classical impulse approximation.

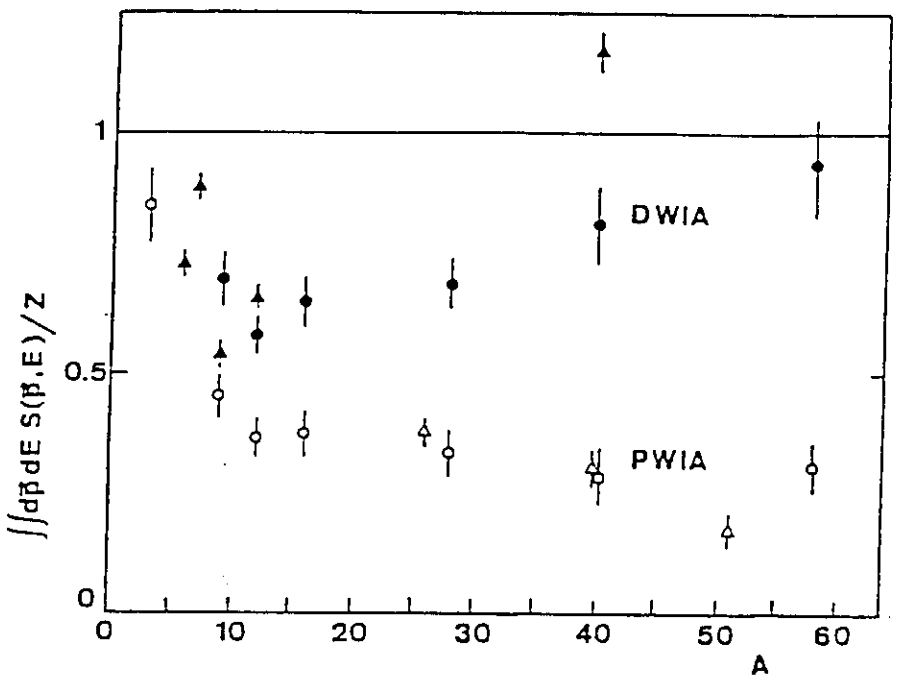

Figure 8 (e,e'p) results for the spectroscopic sum rule (from ref. 13).

Direct evidence for two–nucleon contributions to the (e,e'p) reaction cross section has been obtained at Saclay[15] on ^3He (figure 9) at large ω and p_m values (towards the "dip" region). The narrow peak around 5 MeV is associated with the two-body (pd) break up. The broad structure which moves towards higher E_m value with increasing p_m value results [16] from an interaction with a correlated (n p) pair. The energy shift follows the kinematics for the d(e,e'p)n reaction, the width of the peak being related to the motion of the pair in the ^3He nucleus. It is worth noticing that, at the highest p_m value of 458 MeV/c, this contribution dominates over the "one body" contribution seen at E_m=5MeV, showing clearly that high momentum components in nucleon wave functions arise mainly from strong two-nucleon interactions. Similar observation has been done at Bates on ^{12}C, in the "dip" [17] and Δ–peak [18] region. Figure 10 shows that the cross section near the Δ–peak can only be explained if a substantial contribution of two-nucleon emission processes is added to the quasifree Δ production with pion emission. These results are very similar to those of Homma et al [19] using real tagged photons in $^{12}C(\gamma,p)$ reactions.

Like in inclusive (e,e') scattering, deeper insight in the (e,e'p) process is obtained if one separate transverse and longitudinal contributions. At present, very few experimental results are available, but they tend to confirm the quenching of the longitudinal response observed in inclusive experiments. Here, direct two nucleon emission is eliminated, by selecting bound nuclear final states. Provided final state interactions are properly treated, one should be sensitive to possible modifications of the nucleon electromagnetic response (currents, form factors, ...) in the nuclear medium.

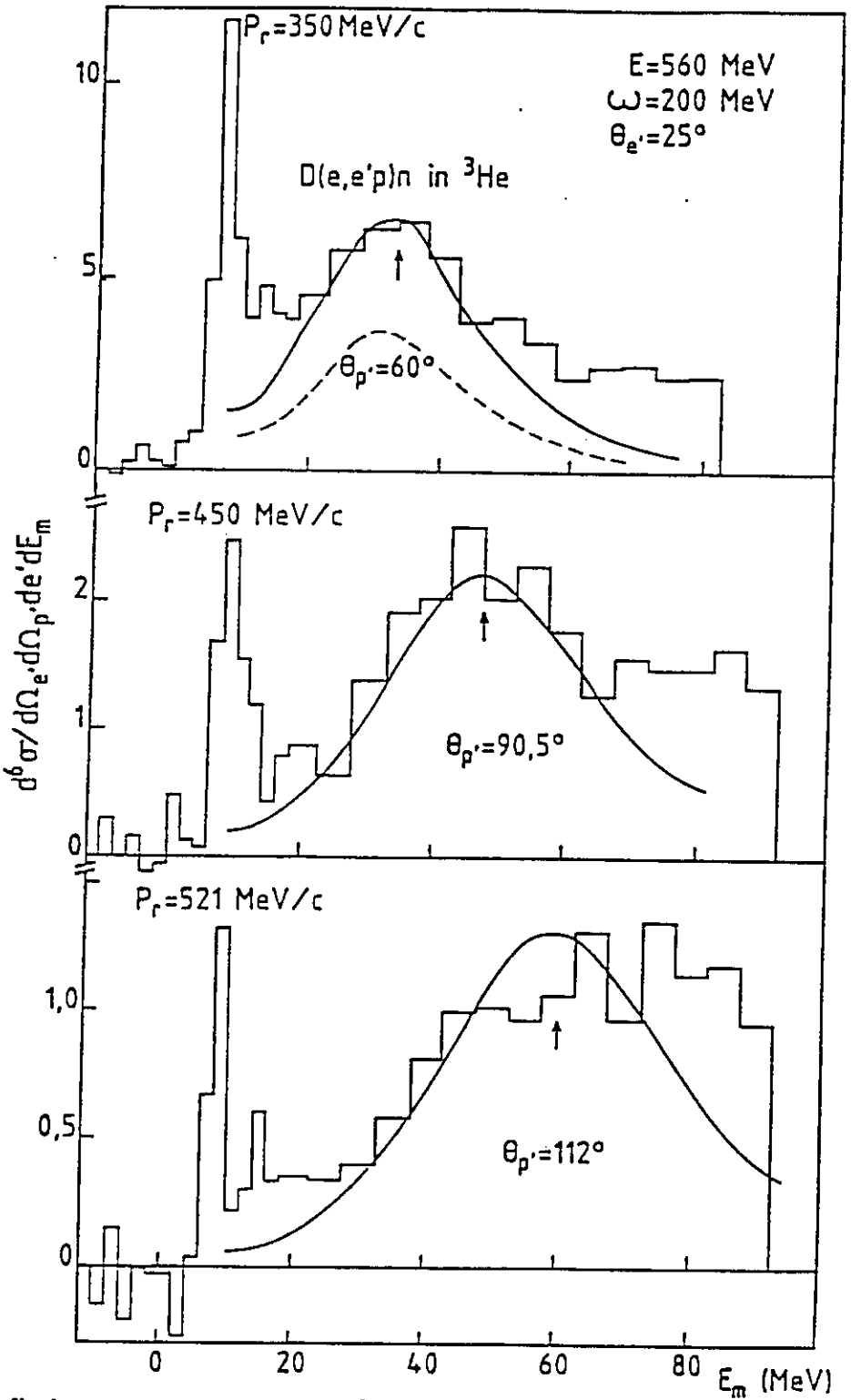

Figure 9 Missing energy spectra from ^{3}He(e,e'p) showing evidence for an interaction on a two-nucleon correlated pair (from ref. 15).

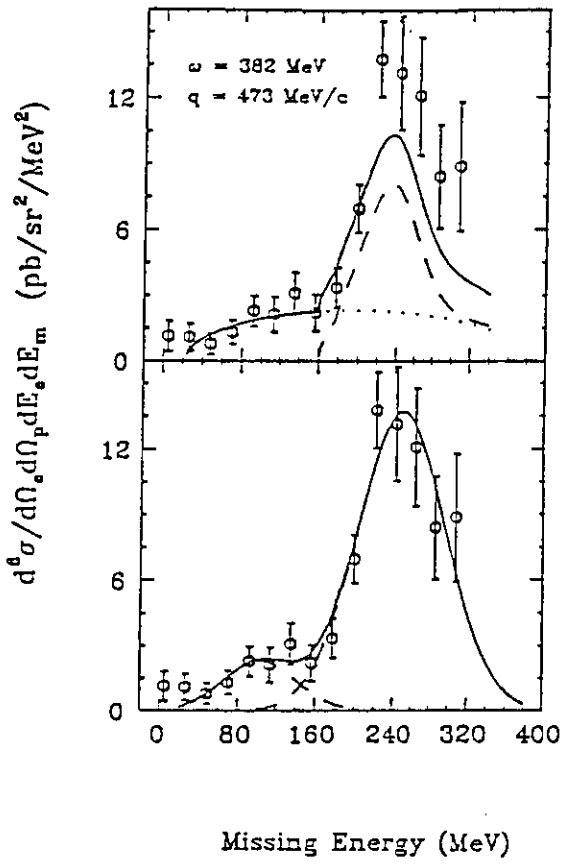

Figure 10 Missing energy spectrum from ^{12}C(e,e'p) at the top of the Δ-quasifree peak. Upper curves show the contributions from (– – –) quasifree pion production, (.....) two-nucleon emission phase space, (——) total. Lower curves are gaussian fits centered around (– – –) quasideuteron breakup and (——) Δ-quasifree peak (from ref. 18)

Figure 11, from NIKHEF [20] on $^{12}C(e,e'p)^{11}B$ and figure 12 from Saclay [21] shows a 20-30% deviation in the ratio G_E^2/G_M^2 for a bound nucleon compared to the free one, when the reaction is interpreted within PWIA or DWIA. Care was taken by both groups of possible "differential" FSI and Coulomb distortions in the DWIA analysis. However, no marked deviation in the Q^2 dependence of this ratio is observed, within the (limited) Q^2 range studied. Obviously, one needs a considerable improvement in experimental precision as well as a large range of kinematic variation to demonstrate any effect related to nucleon modifications in the nuclear medium.

As we have seen on these few examples, (e,e'N) reactions can address a very rich variety of physics issues, from single nucleon densities and two–nucleon short range effects to multi quark cluster phenomena and nucleon electromagnetic properties in nuclear medium. A fully quantitative interpretation generally implies the separation of the various response functions. In most cases, it is crucial to study the Q^2 dependence of the cross sections over a broad Q^2 range, as nucleon internal degrees of freedom do play a role in nucleon emission processes at high Q^2. Moreover, some of these studies require high to very high (missing) energy resolution, when nuclear structure aspects are investigated, or to use the nucleus as a spin, isospin or density filter. This calls clearly for electron accelerators with 100% duty–cycle, high (a few GeV) incident energy, high beam qualities (allowing high resolution work at high luminosity) and equipped with high resolution and large acceptances detection systems.

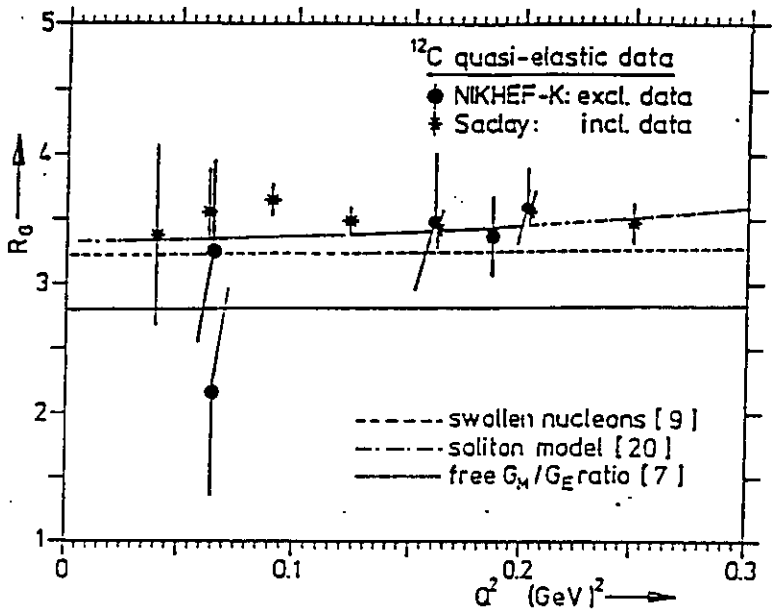

Figure 11 Ratio of transverse and longitudinal structure functions for ^{12}C(e,e'p) interpreted as the value of G_M^2/G_E^2 inside the nucleus (from ref. 20)

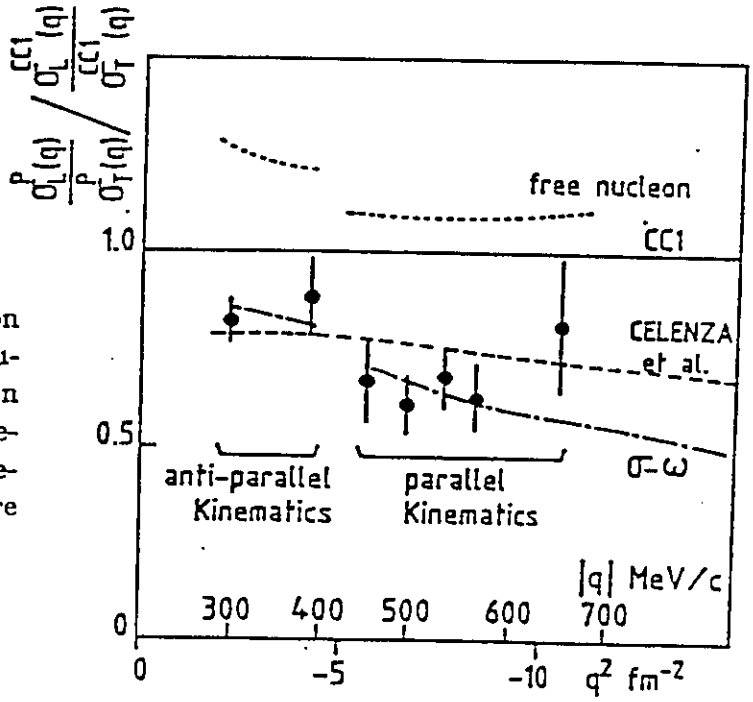

Figure 12 Ratio of σ_L^p/σ_T^p for a proton bound in ^{40}Ca compared to (.....) free nucleon ratio (-.-.) $\sigma-\omega$ model prediction (- - -) non-topological soliton model prediction. The ratio is normalized to DeForest σ_{CC1} prescription (47). Data are from ref. 21

III. Separation of the Nuclear Responses

As most of the (e,e'N) experiments to be performed with the new generation of continuous electron beam accelerators will imply a separation of the different structure functions in the nuclear response, we recall briefly the general formalism for coincidence (e,e'X) reactions in the one–photon–exchange approximation. More detailed developments can be found in refs. 22-26

Taking as an example the $\vec{A}(\vec{e},e'N)B$ reaction with polarized beam and target (see figure 13, also for notations) it follows from general invariance arguments that the one–photon–exchange cross section depends upon nine structure functions and can be written as

$$d\sigma/d\vec{e}'d\vec{p}' = (\alpha^2/Q^2)\,[e\ e'R(1-\epsilon]^1\,.[\Sigma + h\Delta] \tag{4}$$

with

$$\begin{aligned}\Sigma &= 2\epsilon_\ell f_{oo} + f_{11} + \sqrt{\epsilon_\ell(1+\epsilon)}\,(f_{01}\cos\alpha + \bar{f}_{01}\sin\alpha) \\ &\quad - \epsilon_\ell\,(f_{1-1}\cos 2\alpha + \bar{f}_{1-1}\sin 2\alpha) \\ \Delta &= \sqrt{1-\epsilon^2}\,\bar{f}'_{11} + \sqrt{\epsilon_\ell(1-\epsilon)}\,(f'_{01}\sin\alpha + \bar{f}'_{01}\cos\alpha)\end{aligned} \tag{5}$$

h being the incident electron helicity value (± 1), and ϵ, ϵ_ℓ the photon polarization parameters

$$\epsilon = \left[1 + 2(\vec{q}^2/Q^2)tan^2\theta/2\right]^{-1} \qquad \epsilon_\ell = \epsilon.Q^2/\vec{q}^2 \tag{6}$$

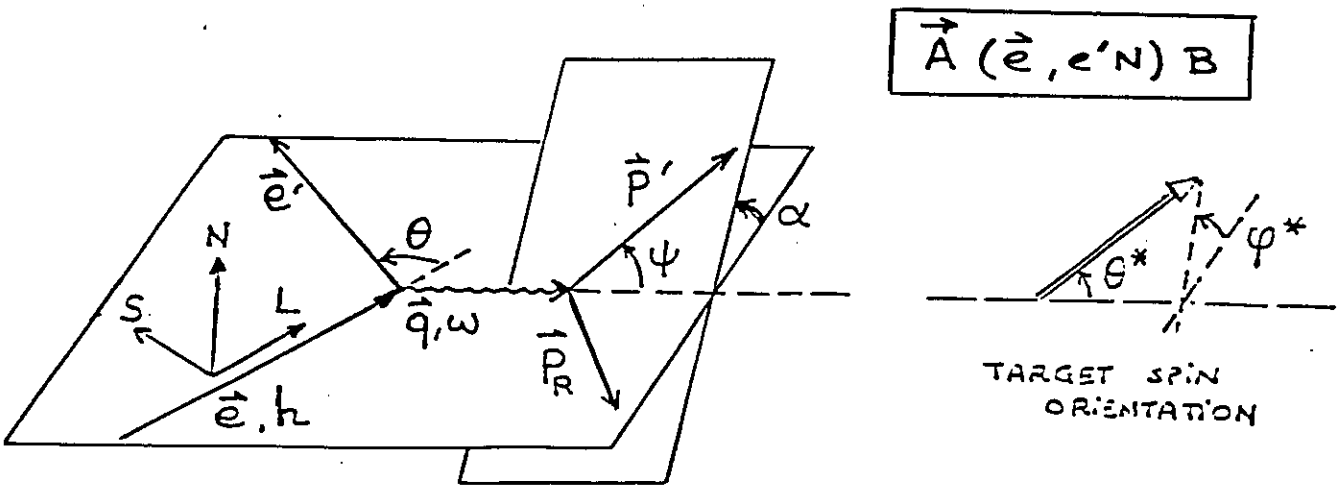

Figure 13 Kinematical notations for the $\vec{A}$, ($\vec{e}$, e'N)B reaction.

The nine Lorentz invariant response functions f_{ij} depend on six kinematical parameters, usually taken as ω, q, p', $\gamma = (\vec{p}', \vec{q})$ and the target spin orientation angles θ^* and ϕ^*.

The dependence upon α, the angle between the hadron emission plane and the electron scattering plane is simple, and given explicitly. By varying the other kinematical variables – like the incident energy e, the electron scattering angle $\theta, \ldots$ – keeping the relevant ones constant, one can in principle separate the various response functions. All $\bar{f}_{ij}$ vanish if the target is unpolarized, reducing the number of response functions to five, and even four if the beam is also unpolarized (all $f'_{ij} = 0$). One can show that the so-called "fifth" structure function f'_{01} does not contribute in PWIA but can contribute only when other reaction channels are included in the calculation, as in DWIA. This is one –among many– example showing that particular reaction mechanisms involving specific dependence on external variables will translate into specific sensitivity of each response function which can be enhanced under appropriate kinematics.

More structure functions can be obtained if the polarization of the outgoing nucleon is measured [25]. All these structure functions are bilinear products of the matrix elements of the nuclear current J_μ which are conveniently written in terms of helicity amplitudes (see table I as an example). The number of amplitudes – thus the number of independent measurements required – clearly depends on the spins S_A, S_x and S_B, and if the spins are not too large it may be possible to measure all of these amplitudes (up to an overall phase) and to completely determine the electro disintegration process. For instance, for the ^3He (e,e'p) np reaction at low (np) relative energy (^1S_o final state) there are only 6 different helicity amplitudes, requiring 11 independent measurements.

The sensitivity of the various responses is illustrated in figures 14 and 15. Figure 14 is from a relativistic mean field calculation of Picklesimer et al.[25] on $^{16}O(\vec{e}, e'p)^{15}N_{g.s.}$, in which one sees the sensitivity of the interference functions R_{TT} and $R_{LT'}$, (respectively f_{1-1} and f'_{01}) to the offshell character of the T-matrix describing final state interaction. Figure 15, from Boffi et al. [26] on $^7\vec{L}i(\vec{e}, e'p)^6He_{g.s.}$ shows that, for polarized targets, the fifth structure function f'_{01} can be as large as the usual longitudinal (f_{00}) and transverse (f_{11}) ones.

IV. One-Body Densities From (e,e'N) Reactions

As shown in section II, the (e,e'N) data presently available have been taken essentially around the quasielastic peak, where cross sections are high.

Although some systematics exist, the kinematical domain explored is very limited (low p_m, low E_m), the statistical accuracies are often poor, and very few results are obtained on separated responses. Major progresses are expected from continuous electron beams below 1 GeV, which will be available at University of Illinois, Mainz, NIKHEF and hopefully at Bates.

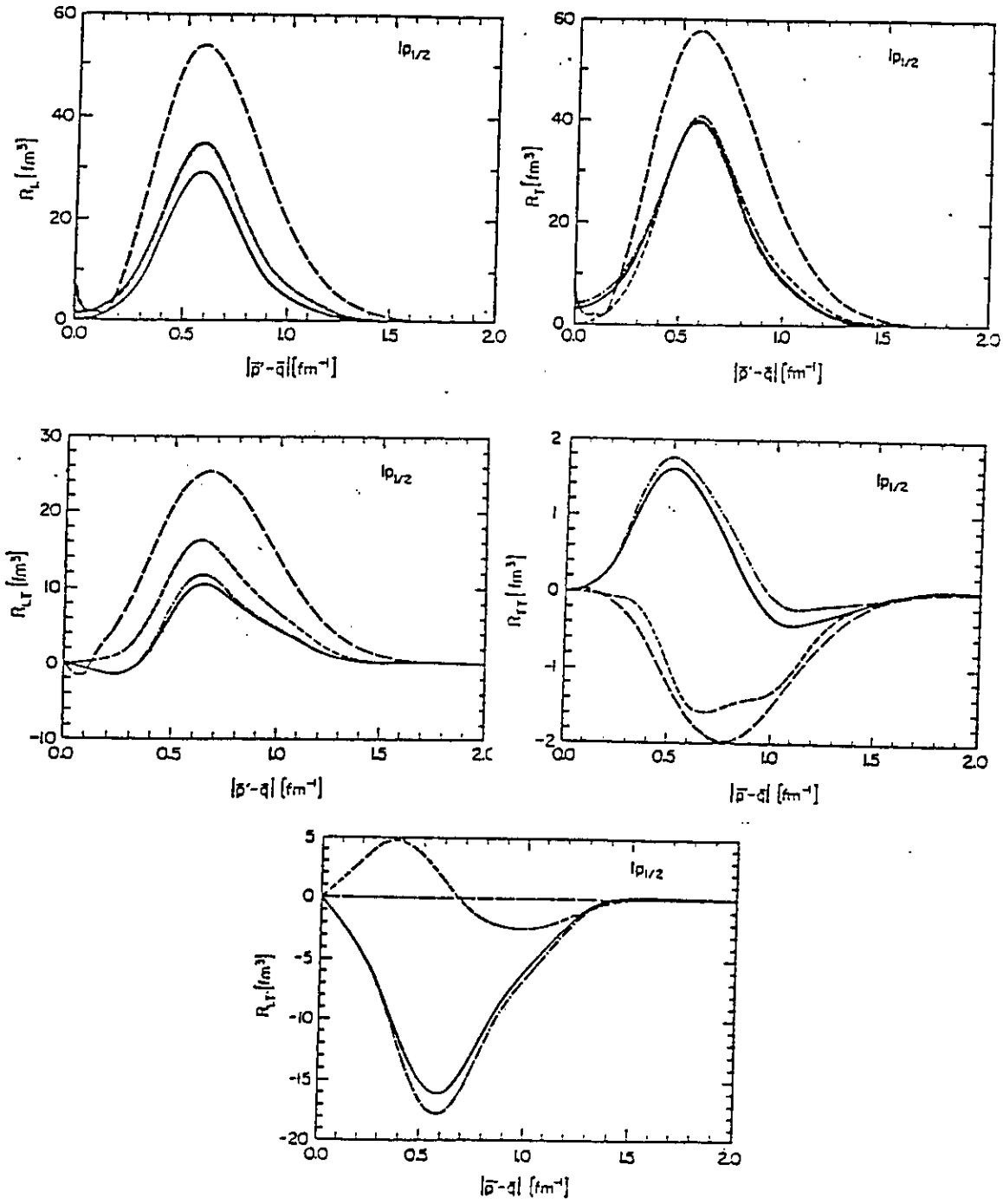

Figure 14 Relativistic mean field calculation of the five response functions for the $^{16}O(\vec{e}, e'p)^{15}N$g.s. reaction (– –) plane wave (–.–.–) non relatisvistic Schrodinger bound and final state (– – –) on-shell relativistic result (——) off-shell relativistic result (from ref. 25).

Table I

Lorentz invariant response functions f_{ij} (see eq. 5)

$$f_{oo} = \mid J_o \mid^2$$
$$f_{11} = \mid J_1 \mid^2 + \mid J_{-1} \mid^2$$
$$f_{01} = 2Re\left(J_1 J_o^* - J_o J_{-1}^*\right)$$
$$f_{1-1} = 2Re(J_1 J_{-1}^*)$$
$$\bar{f}'_{11} = \mid J_1 \mid^2 - \mid J_{-1} \mid^2$$
$$f'_{01} = -2Im(J_1 J_o^* + J_o J_{-1}^*)$$

$$\bar{f}_{01} = -2Im(J_1 J_o^* - J_o J_{-1}^*)$$
$$\bar{f}_{1-1} = -2Im(J_1 J_{-1}^*)$$
$$\bar{f}'_{01} = 2Re(J_1 J_o^* + J_o J_{-1}^*)$$

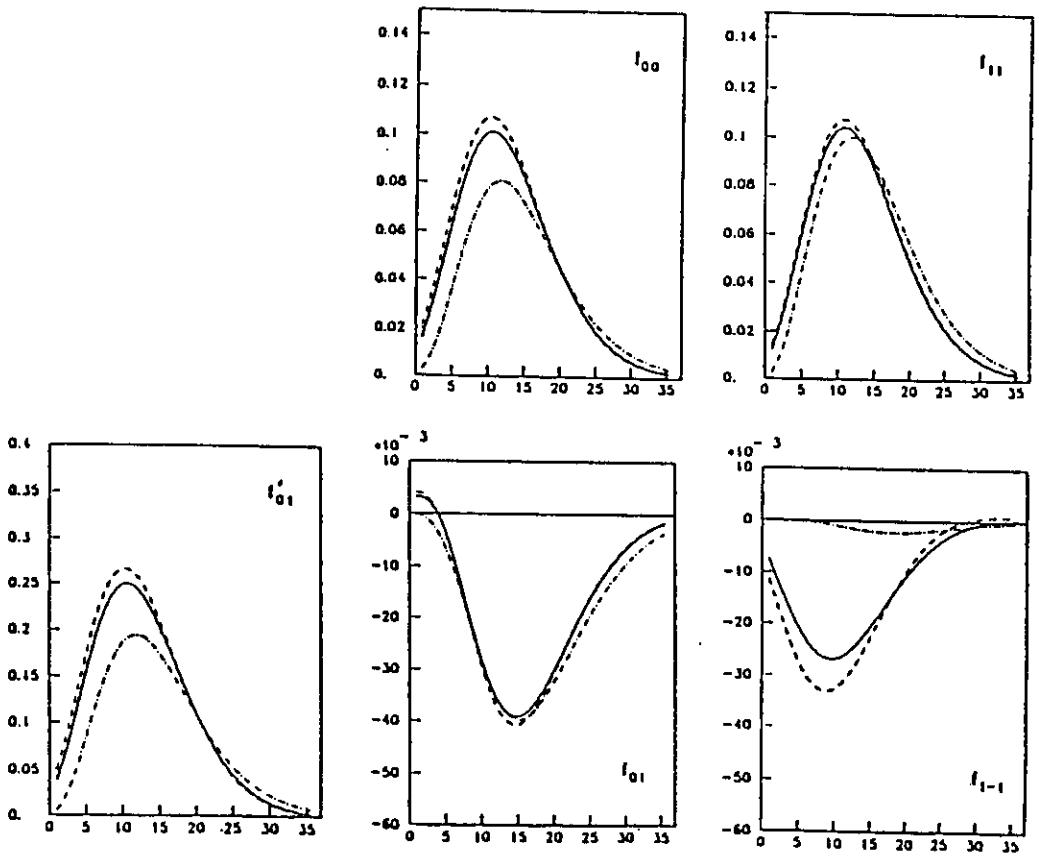

Figure 15 Response functions for the $^7\vec{L}i(\vec{e}, e'p)\ ^6He_{g.s.}$ reaction at 700 MeV (–.–.–) plane wave; (—) and (– – –) distorted wave calculations (from ref. 26).

However, higher incident energies, like the 4GeV CEBAF designed value, bring several advantageous features:

- larger cross sections at a given Q^2 (see figure 16)
- wider Q^2 range
- higher kinematical flexibility for separations, in particular large $\Delta\epsilon$ lever arms. (see figure 17)

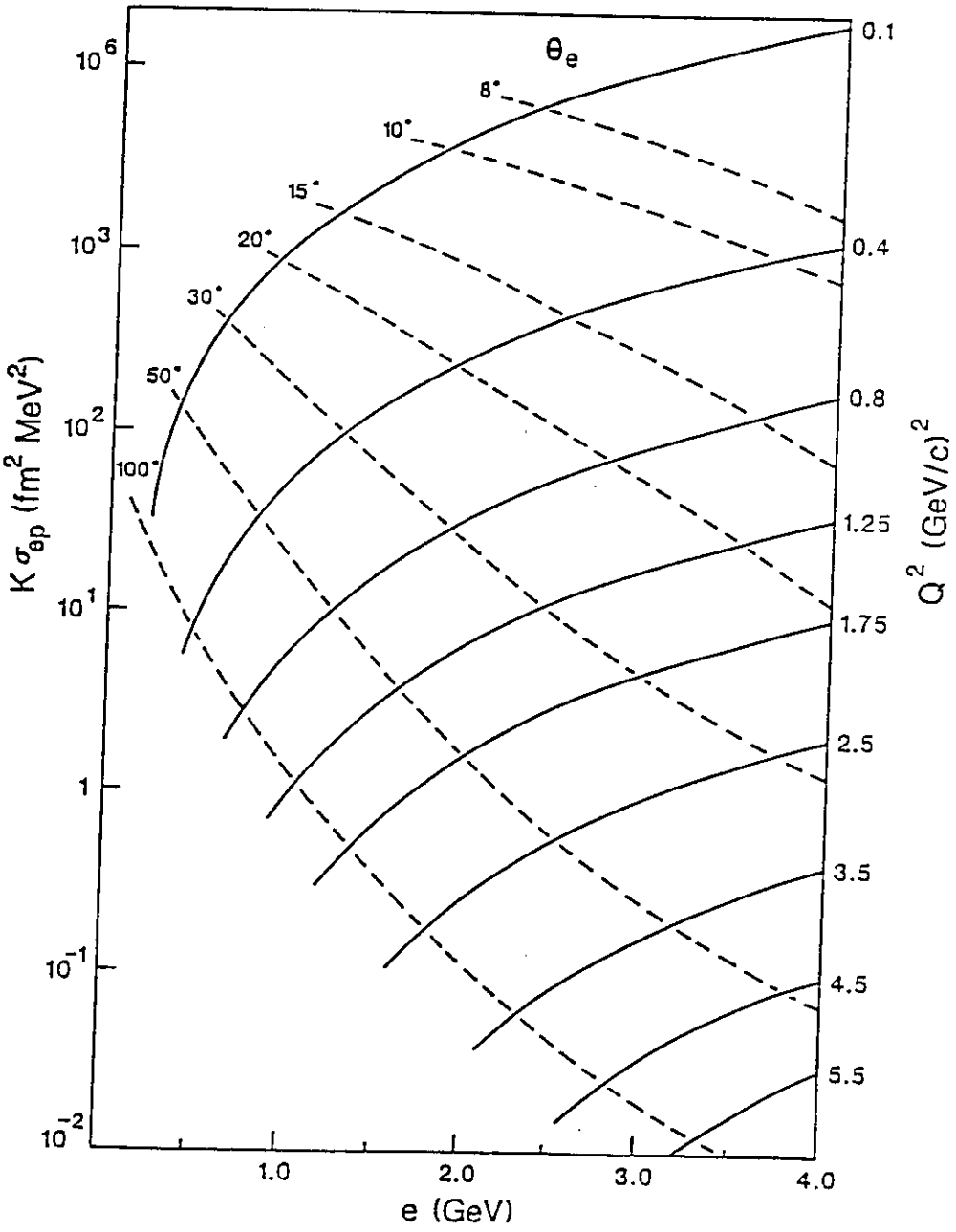

Figure 16 The quantity K σ_{ep} (see eq. 1) as a function of the incident electron energy for the reaction ^{12}C(e,e'p)^{11}B at different Q^2 values.

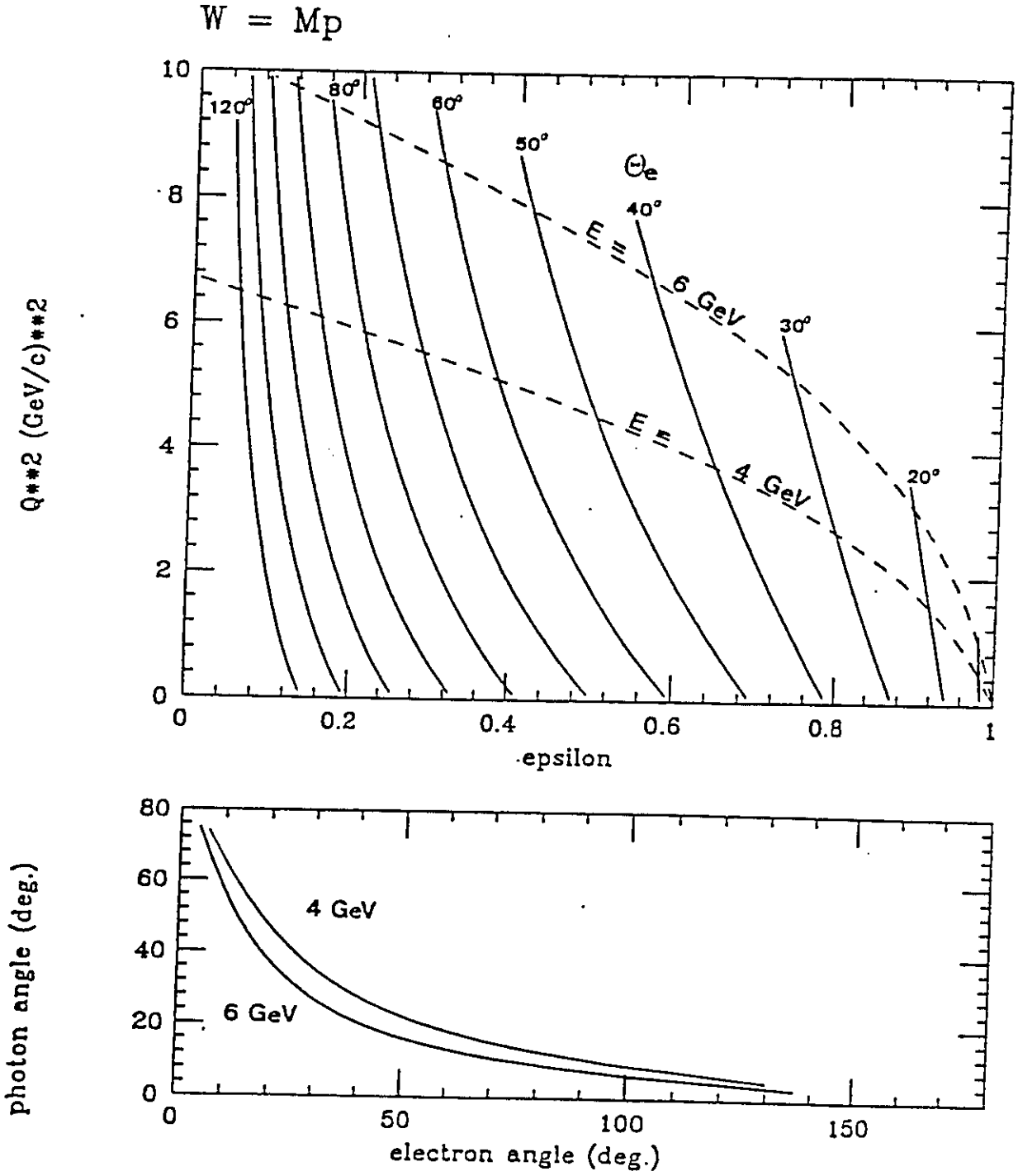

Figure 17 Kinematical domain accessible for longitudinal/transverse separations at the quasielastic peak.

One should note in passing that, although there is a shallow minimum in the total p-nucleus reaction cross section between 200 and 400 MeV, (see figure 18, from ref. 57) FSI are not expected to be dramatically worse at higher energy.

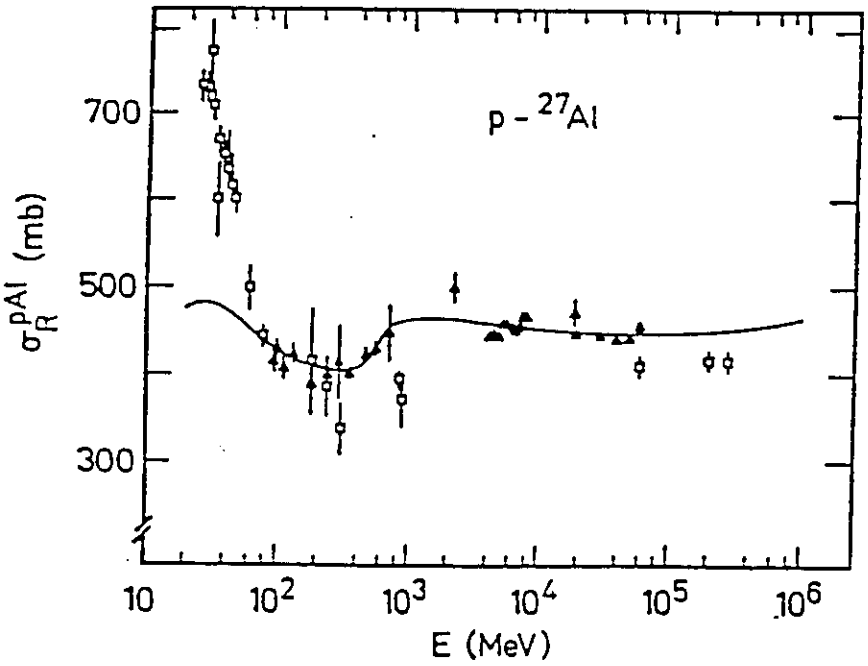

Figure 18 Total p-^{27} Al cross section (from ref.57)

The expected improvement (~100) in cross section sensitivity from the high duty cycle and beam intensity available at the new facilities should allow to perform (e,e'n) as well as (e,e'p) experiments. Figure 16 shows that (e,e'n) cross sections are typically one order of magnitude smaller at low Q^2, but only a factor of 2–3 above $\sim 1(\mathrm{GeV/c})^2$. For (e,e'p) reactions, the increased sensitivity should allow to map density distributions to much higher p_m(>600 MeV/c) and E_m (>100 MeV) values, in new regimes where new structures may show up. High resolution will allow to map out the density in momentum space for natural parity (hole) and unnatural parity (multi particle – multi hole) states of many different spins and isospins. Separations of the various response functions, in particular of the interference ones, will give deeper insights on some specific nuclear physics issues. As an example, detailed studies of momentum density distributions for spin–orbit partner hole states ($\ell \pm \frac{1}{2}$) at low and high $p_m$values should deepen our understanding of the origin of the spin-orbit force.

An important part of this program is likely to be the complete study of the electro-disintegration of few nucleon systems. (A≤4). They combine several advantages: most of the effects discussed previously are present, as they cover a substantial range of nucleon binding energies and nuclear densities. Due to their relatively simple structure, nearly exact calculations for various reaction channels can be performed. Moreover, they allow to perform completely exclusive experiments without resorting to extremely high resolution (typically ~ 1MeV would be needed, to separate bound deuterons from unbound (np) pairs).

Deuteron electrodisintegration is the first obvious candidate. Although it is the simplest nucleus, deuteron remains a puzzle, some pieces of which being shown in figure 19. Difficulties remain in explaining the elastic structure function A (Q^2) at high Q^2 (figure 19a) in terms of two-nucleon relativistic wave functions, using the most recent two-nucleon forces. Theoretical curves[27] are below experimental data by an order of magnitude, unless the nucleon form factors (mainly the poorly known G_E^n) are modified according to Gari and Krümpelmann [30] leading to $G_E^n > G^nM$ above $Q^2 = 4$ $(GeV/c)^2$ (see figure 20). The new data[28] for the magnetic elastic structure function $B(Q^2)$ shows a diffraction minimum around $2(GeV/c)^2$, coherent with a two–nucleon description of the deuteron at these momentum transfer values, but departing strongly from what can be expected from quark model predictions. As it is well known, the separation of the charge G_C and quadrupole G_Q form factors, both combined with G_M in $A(Q^2)$, requires the measurement of a polarization observable. At present, our knowledge of t_{20} – considered to be the most promising one – is very poor. Figure 19c (from ref. 29) shows that above $Q^2 = 0.5$ $(GeV/C)^2$ – a totally unexplored region – the theoretical predictions differ very strongly!

A complete study of the electrodisintegration of three body systems will have also to be performed. Exact Faddeev [33] and variational [34] calculations for ^3He and ^3H ground state wave functions are available, allowing to derive the one–nucleon spectral function $S(p_m, E_m)$. Faddeev caluclations in the continuum are underway [35]. The systematic studies of (e,e'p) and (e,e'n) reactions on ^3He and ^3H will allow to separate the two isospin components (T = 0 and 1) of the one–nucleon spectral function in A = 3 systems. (see figure 21). Note that, assuming charge invariance of nuclear forces and neglecting Coulomb effects, one has

$$\begin{aligned} S_p^{^3He} &= 3S_{T=0} + S_{T=1} = S_n^{^3H} \\ S_p^{^3H} &= 2S_{T=1} \qquad\quad = S_n^{^3He} \end{aligned} \tag{7}$$

Of particular interest in the study of the high momentum components in the ^3He wave function. From three nucleon calculations, it can be shown that the high p_m values in the one–nucleon spectral function are associated with high values of E_m (see figure 22, from Ciofi et al., ref. 34), i.e. high relative energy values for the residual (np) pair. Such correlation is coherent with the experimental observation of ref. 15.

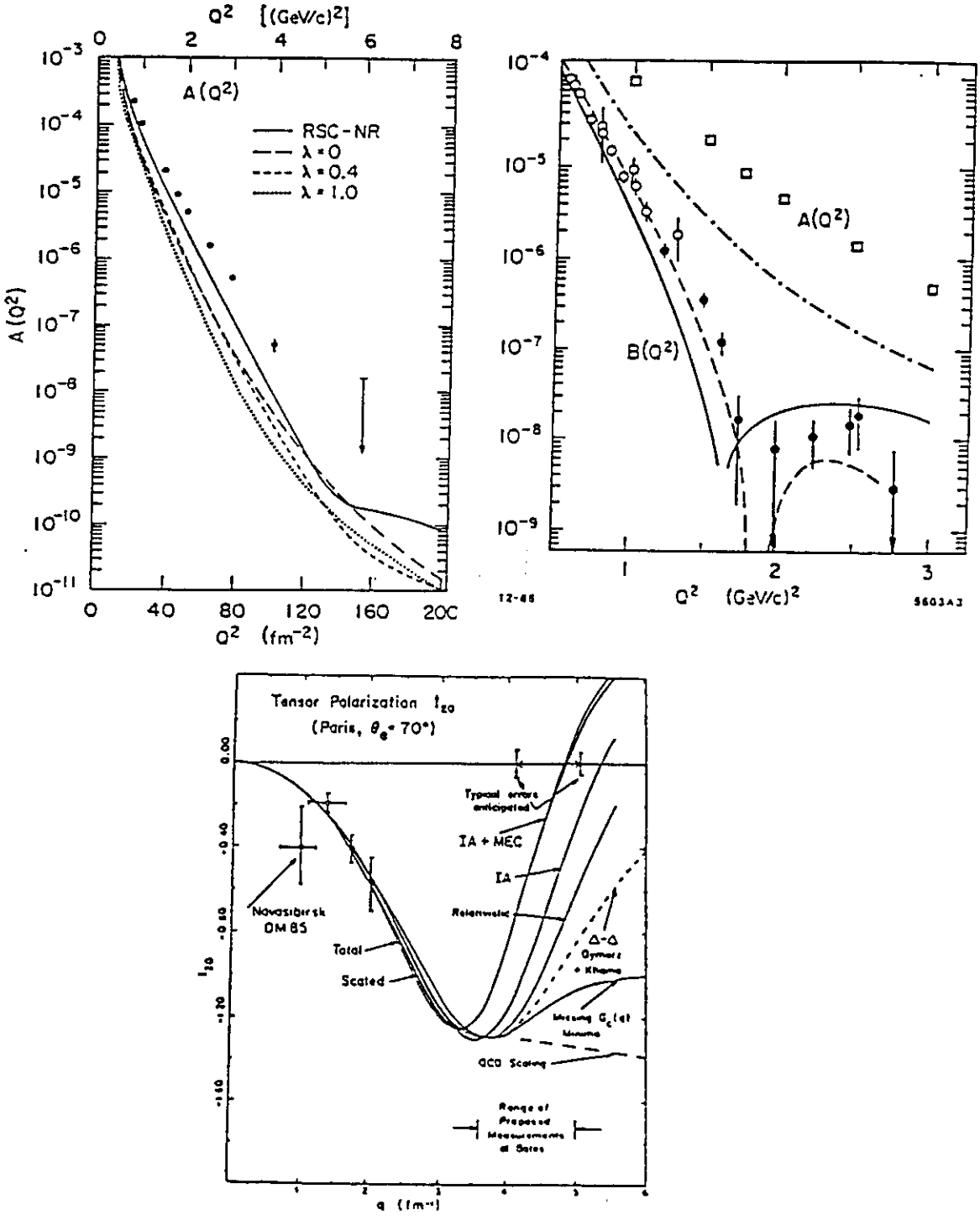

Figure 19 Some pieces of the deuteron puzzle (see text).

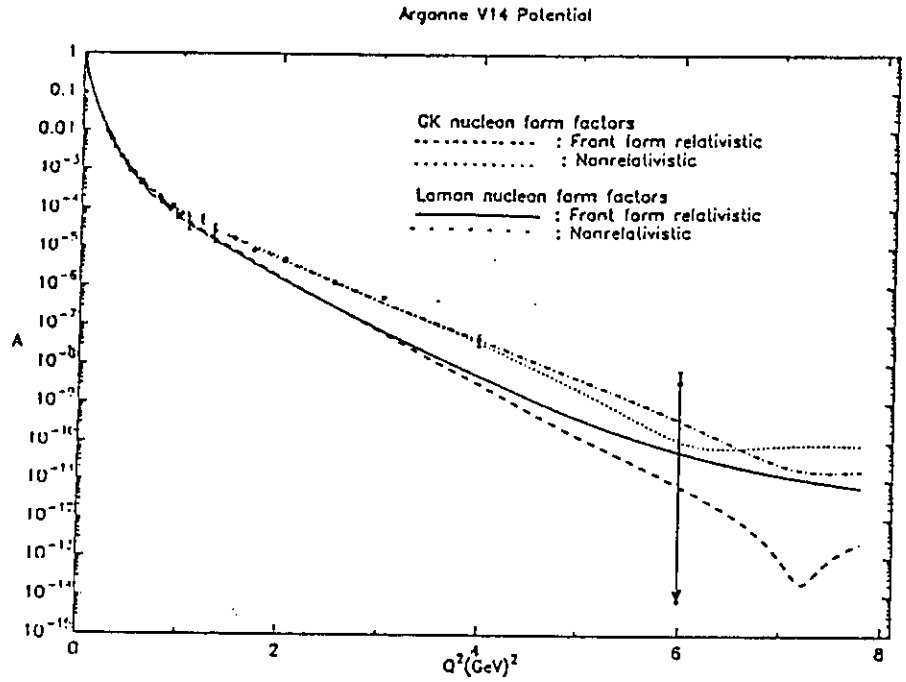

Figure 20 Relativistic calculations for the deuteron elastic response function $A(Q^2)$ (from ref. 31 and 32).

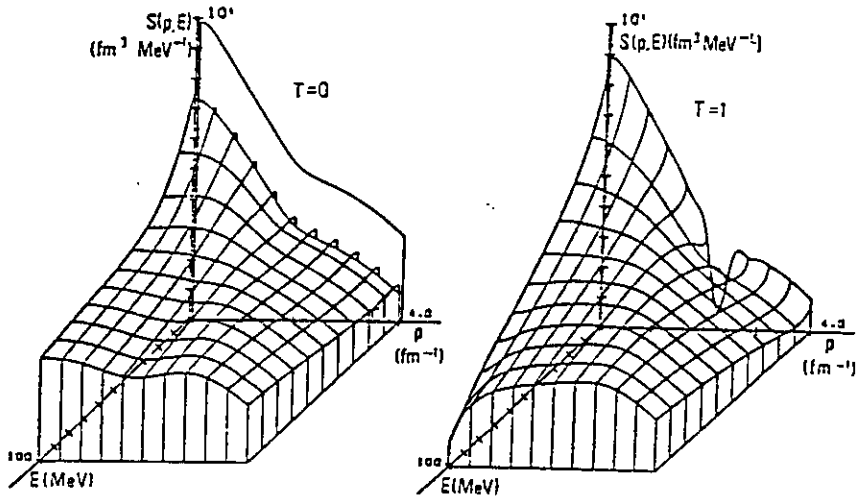

Figure 21 ^{3}He spectral function from Meier-Hadjuk et al., (ref. 33). Contributions arising from correlated pairs in the final state with isospin T=0 (left) and T=1 (right) are show separately.

Calculations have been made under CEBAF experimental conditions [36] to determine the p_m ranges within which (i) the ^3He spectral function can be measured (ii) the various (unpolarized) structure functions can be measured. Results are shown in figures 23 and 24 together with the assumed values for luminosities and acceptances. At forward electron angle, the two body (pd) break up can be followed up to $p_m \sim 800$ MeV/c with a few counts/hour. However, at these high momentum values, the experimental cross section will be dominated by the complete 3-body disintegration. Separations can be performed up to $p_m \sim 600$ MeV/c, at least for the three dominant (in-plane) structure functions. A critical issue will be the reduction of systematic errors to the level of 1 –2%.

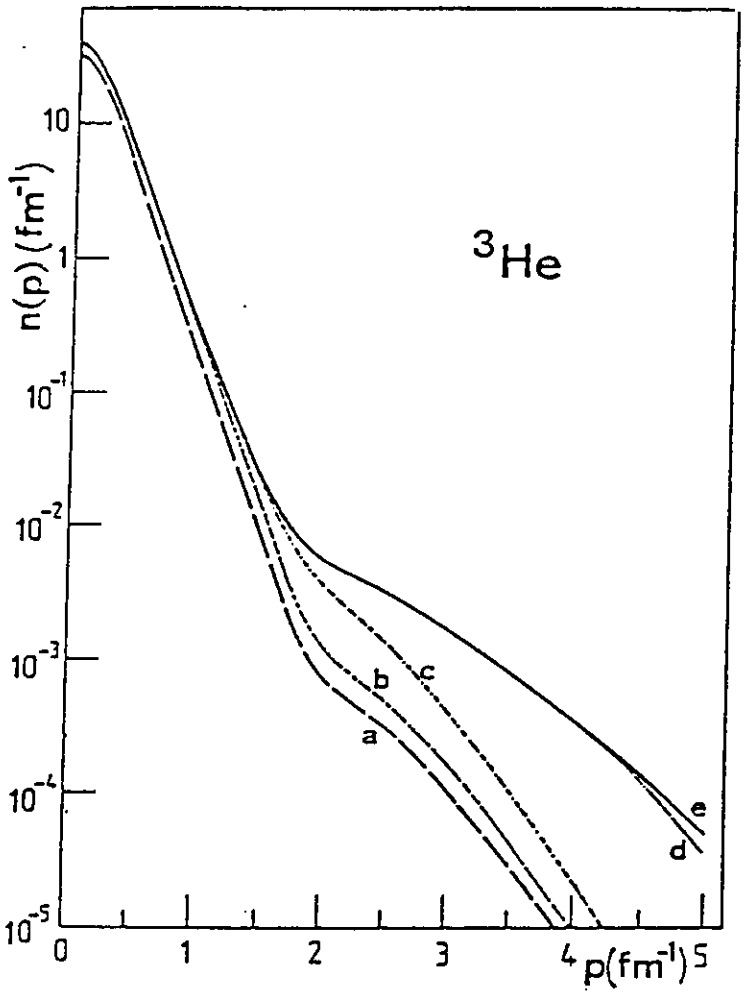

Figure 22 The proton momentum distribution in ^{3}He: (a) two-body break-up; (b)(c)(d) calculated by integrating $S(p_m, E_m)$ up to E_m = 12.25, 50 and 300 MeV respectively, (e) total (from Ciofi degli Atti, ref. 34).

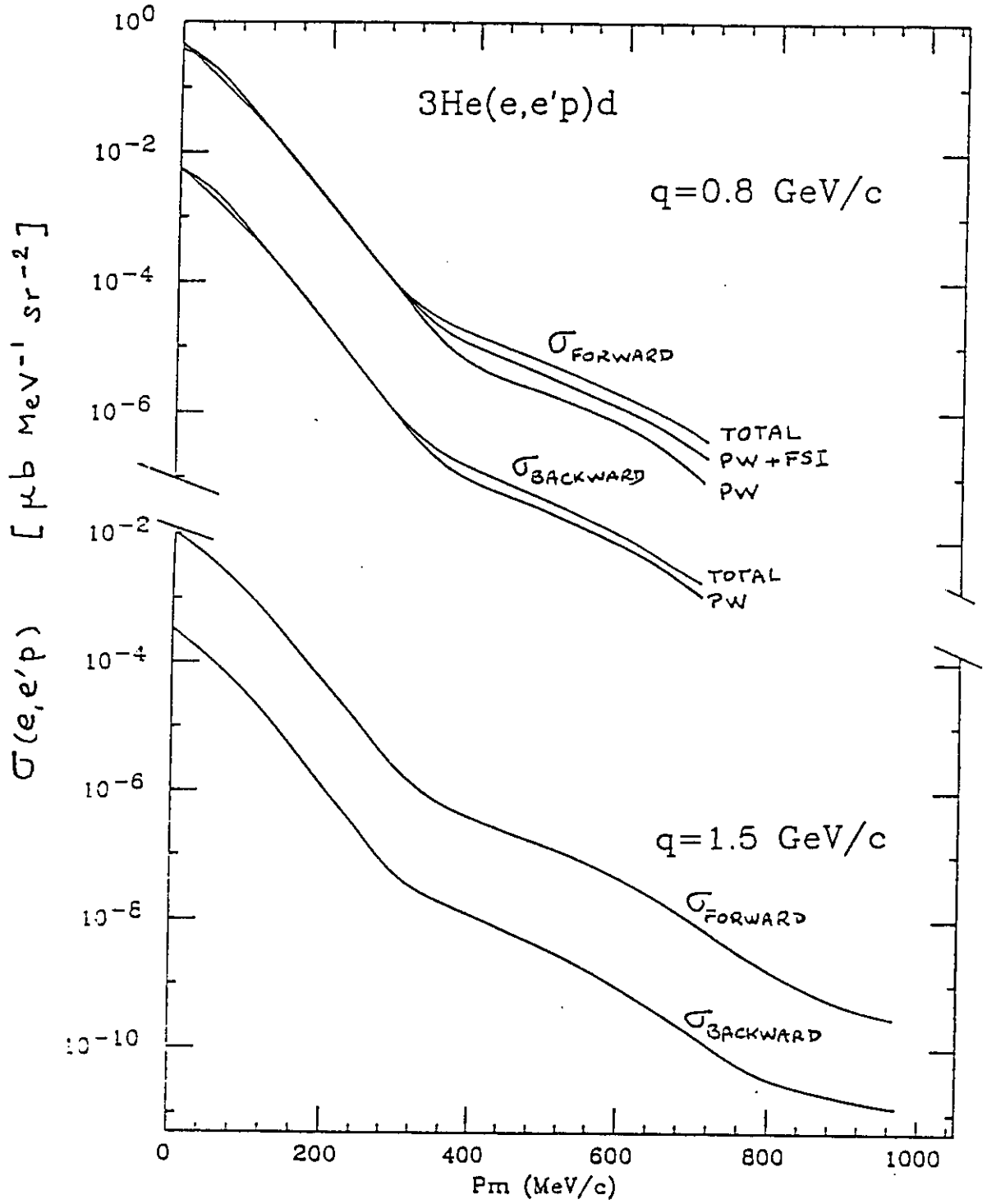

Figure 23 ^{3}He(e, e′ p) d reaction cross section at $|\vec{q}| = 0.8$ and 1.5 GeV/c.

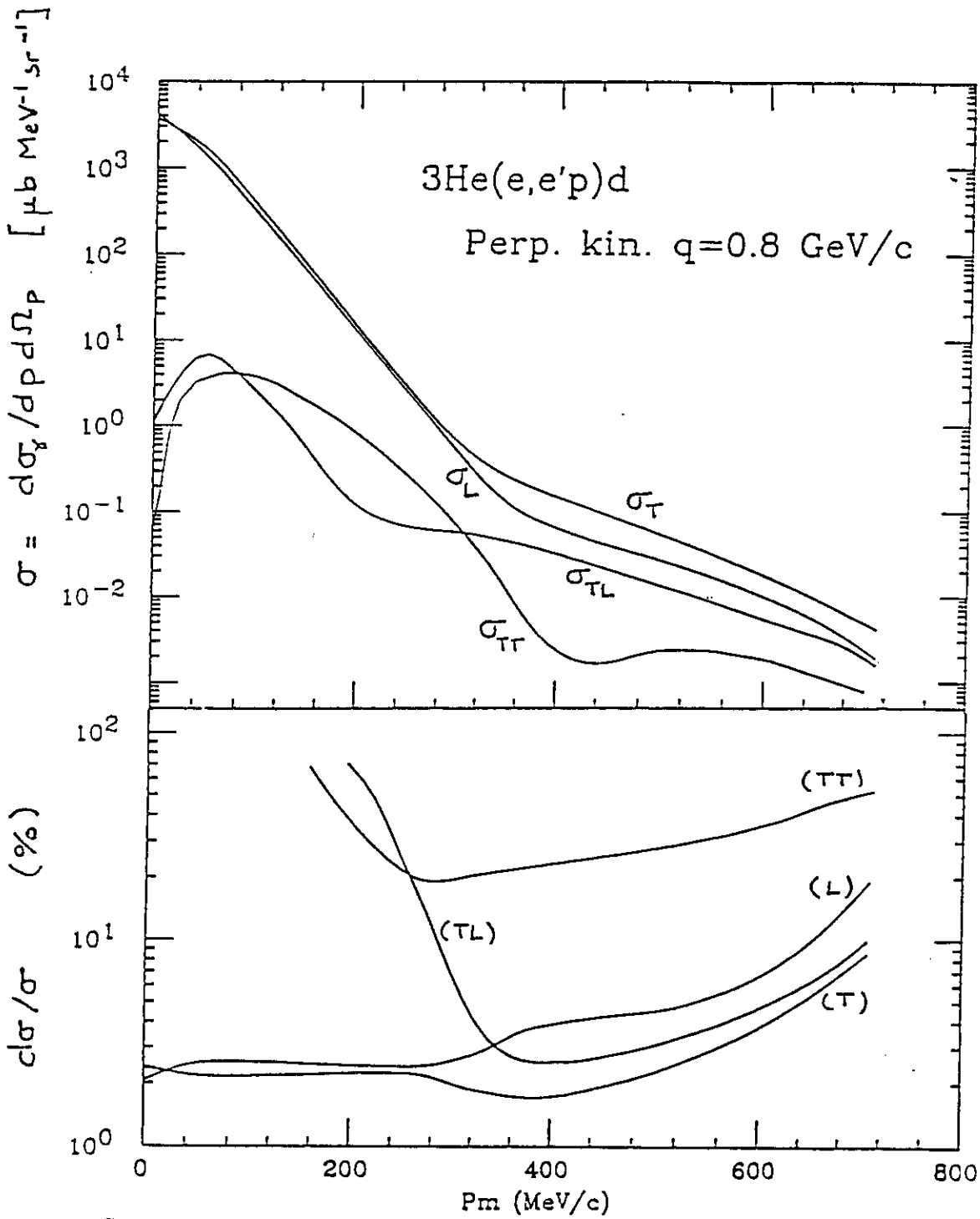

Figure 24 Separation of the various response functions for the ^{3}He(e, e′ p)d reaction at $|\vec{q}| = 0.8$ GeV/c. Relative uncertainties were determined assuming CEBAF spectrometer acceptancies ($\Delta\Omega_e = \Delta\Omega_p = 10msr, \Delta e'/e' = \Delta p'/p' = 10\%$) a luminosity value of 10^{36} cm^{-2} sec^{-1}, 2% systematic uncertainties and a limitation of 100 hrs per kinematical point.

V. (e,e'd) and (e,e'2N) Reactions

Coincidence studies of two–nucleon emission processes like (e,e'd) and (e,e'2N) provide the most direct access to two-nucleon densities and correlation functions in nuclear medium. These basic quantities are of fundamental importance. Two nucleon densities are necessary inputs in meson exchange current calculations. At short distances, they should give insights on two–nucleon clustering in nuclei – exchange of heavy mesons ($\rho, \omega \ldots$), 6-quark clusters, ... – and on the origin of high momentum components in nuclear wave functions.

Table 2

Counting rates for ^3He(e,e'2p)n and ^3He(e,e'pn)p reactions

Experimental conditions:

$E_e = 2GeV$ $\quad \theta e = 15^\circ$

$\Delta e' = 20MeV$ $\quad \Delta\Omega_e = 10msr$

$\Delta T_1 = 20MeV$ $\quad \Delta\Omega_1 = \Delta\Omega_2 = \Delta\Omega_n = 30msr$

Luminosity = 2.4 x 10^{36} cm^{-2} sr^{-1} $\quad \epsilon_n = 0.1$

Cross sections from Laget, ref. 38

ω (MeV)	θ_1	θ_2	σ_{pp} (pb)	N_{pp}^{true} (hr^{-1})	N_{np}^{true} (hr^{-1})	N_{pp}^{acc} (hr^{-1})	N_{np}^{acc} (hr^{-1})
100	42	102	2.5	261	61	0.9	0.3
200	9	114	0.2	12	48	0.1	0.1
400	-18	104	0.08	5.4	45	<0.1	<0.1
600	-32	92	0.03	1.8	26	<0.1	<0.1

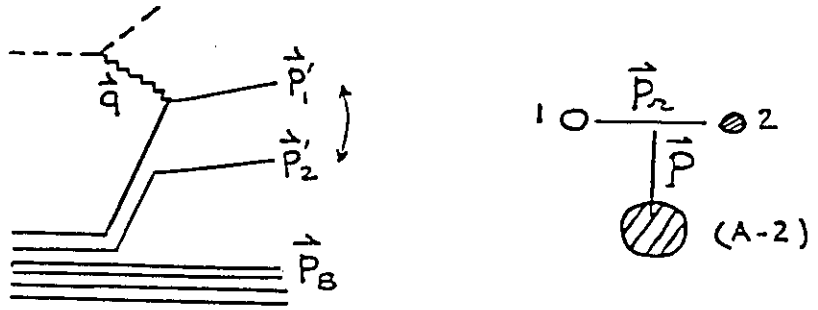

Figure 25 Two-nucleon emission process in PWIA

The simplest process leading to two–nucleon emission is shown in figure 25 (PWIA). One expects intuitively that the associated amplitude will contain two terms, depending upon which of the two nucleons absorb the photon. Schematically, one has the two following situations (see fig. 25 for notations)

$$(I) \qquad \vec{p}'_1 = \vec{p}_1 + \vec{q} \qquad \vec{p}'_2 = \vec{p}_2 \qquad \vec{p}_{r_1} = -\vec{p}'_2 - \frac{\vec{p}_B}{2}$$

$$(II) \qquad \vec{p}'_1 = \vec{p}_1 \qquad \vec{p}'_2 = \vec{p}_2 + \vec{q} \qquad \vec{p}_{r_2} = \vec{p}'_1 + \frac{\vec{p}_B}{2} \tag{8}$$

Consequently, the cross section is written as

$$d\sigma_{PW}\alpha \mid F^{(1)}(Q^2)\phi(\vec{p}_{r_1}, \vec{p}_B) + F^{(2)}(Q^2)\phi(\vec{p}_{r_2}, \vec{p}_B) \mid^2 \tag{9}$$

One can expect that the smallest value of $\mid \vec{p}_{r_1} \mid$ and $\mid \vec{p}_{r_2} \mid$ will gives the dominant contribution. Two particular kinematical choices are worth being mentioned.

a) One can make $\vec{p}'_1 = \vec{p}'_2$. This is the situation for (e,e'd), or (e,e,2N) with $E^{cm}_{NN} \sim 0$ in the final state. Only one spectrometer is required to detect the deuteron or a (2p) pair. One can show that, if ℓ=o dominates for the relative motion of the pair and the (A-2) nucleon residual, one has

$$\phi(\vec{p}_r, \vec{p}_B) \rightarrow f_2(\vec{p}_r)\varphi(\vec{p}_B) \tag{10}$$

In the deuteron case, one has

$$f_2(\vec{p}_r) = \int e^{\,i\vec{p}_r.\vec{r}}\varphi^*_d(\vec{r})\varphi_{np}(\vec{r})d\vec{r} \tag{11}$$

Strong final state interactions occur in the case of an unbound (2p) pair emission in this particular kinematic choice. However, the rescattering occurs mainly in the ^1S_o partial wave, which makes the process simpler.

b) Another choice is $\vec{p}_B = 0$, $\mid \vec{p}'_1 \mid = \mid \vec{p}'_2 \mid$. In this situation, the nucleon pair is emitted at 90° with respect to the photon in the (γ,2N) center of mass system. By varying the momentum transfer and the opening angle, one can vary Q^2 at fixed p_r or p_r at fixed Q^2.

Recent results have obtained at NIKHEF and Saclay for the (e,e'd) reaction on light nuclei. Figure 26 shows results on ^{3}He (e,e'd)p from NIKHEF[37] together with a calculation from Laget which uses free γ.d vertex form factors and an on shell (p.d) t-matrix for FSI. The calculation agrees fairly well with the observed momentum distribution measured at fixed $\mid \vec{q} \mid$ = 380 MeV/c in parallel kinematics. The q–dependence in the range 350-450 MeV/c measured at fixed p_m = 60 MeV/c is also well reproduced, supporting the use of free deuteron form factors. Data on ^{6}Li and ^{12}C are under analysis. Again only limited explorations can be made with presently available beams, and systematic studies including longitudinal/transverse separations are far beyond the present possibilities.

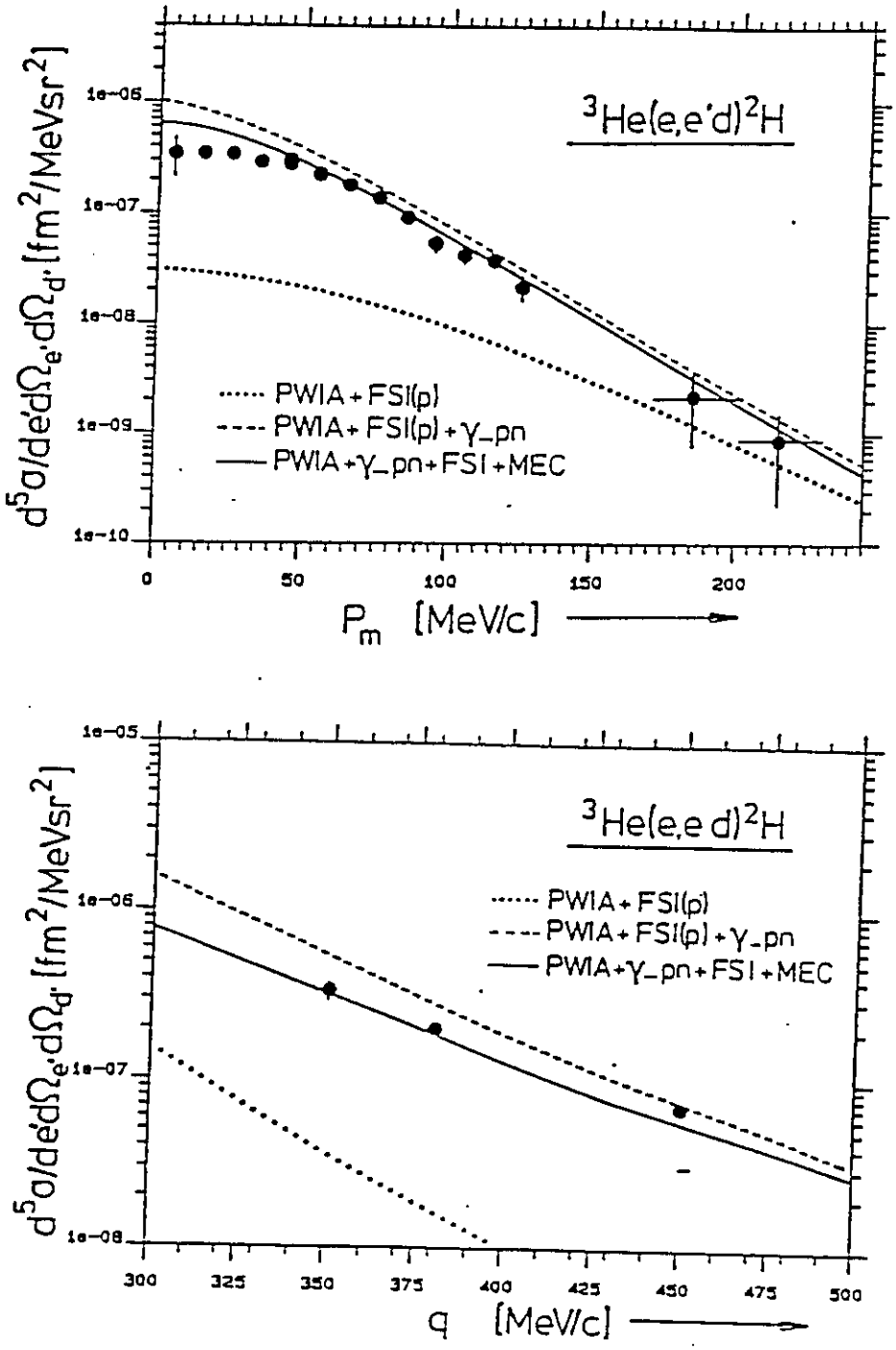

Figure 26 Missing momentum distribution at q = 300 MeV/c (upper) and q-dependence at p_m = 60 MeV/c of the ^{3}He(e,e'd)p reaction cross section (from ref. 37)

The role of correlations, final state interactions and meson exchange mechanisms in the ^{3} He (e,e'2p) n reaction has been investigated recently by Laget [38]. All graphs including two active nucleons have been evaluated, and the transverse and longitudinal part of the cross section

$$\frac{d\sigma}{d\vec{e}d\vec{p}'_1 d\Omega_2} = \Gamma_v . K \left[\sigma_T + \xi\sigma_L + interf.terms\right] \qquad (12)$$

have been separated. The kinematics (E_e = 570 MeV, ω = 200 MeV, $\theta_e = 25^o$, $p_n = 0$) is adapted to the Saclay experimental conditions. The calculation (see figure 27) shows that the transverse part is dominated by meson currents, namely the p$\rightarrow \Delta^+$ transition in the (2p) pair. The plane wave cross section vanishes at $\omega_{cm} = 90^o$ due to a cancellation between the two terms in the amplitude (see formula 9). On the contrary, they add up in the longitudinal part, but the strong (pp) rescattering in S wave modifies totally the plane wave results. One sees also that (pp) pair emission is about two order of magnitude smaller than (pn) pair emission.

Fig. 28, from Laget [38] shows the excitation fucntion of the electrodisintegration of a pp pair at $\theta_{cm} = 90^o$ when $p_n = 0$, in a kinematical conditions (E_e = 2 GeV, $\theta_e = 15^o$) accessible at CEBAF. The comparison with a plane wave result for the longitudinal part - the transverse part vanishes – shows that FSI are very important, even for high values of the relative energy of the two outgoing protons, where Δ–formation make the transverse cross section larger than the longitudinal one.

Counting rate estimates have been performed by Lightbody et al[39] under this kinematics and CEBAF conditions for both (pp) and (pn) detection (see table 2). The use of three spectrometers, or any coplanar arrangement of the detectors, would create difficult topological problems when measuring an excitation function at $\theta_{cm} = 90^o$. A possible arrangement would be the use of one non-focusing spectrometer and one (proton or neutron) time of flight set-up located in a vertical plane containing the momentum transfer $\vec{q}$. Assuming 30 msr solid angles and 20 MeV energy acceptances, reasonable rates for (pn) pairs are obtained for luminosity of 2.4 x 10^{36} cm^{-2} sec^{-1} and a neutron detection efficiency of 0.1, up to $\omega \sim$ 500 MeV corresponding to a relative momentum in the initial pair of $\sim$ 800 MeV/c. However, an auxiliary dipole is required to protect the neutron counters. Although (pp) coincidence rates are substantially smaller, the higher proton single rates may rule out the use of a time-of-flight detection of the second proton. More refined evaluations of the various single rates under different kinematical conditions are necessary before designing the optimal set-up for these triple arm experiments.

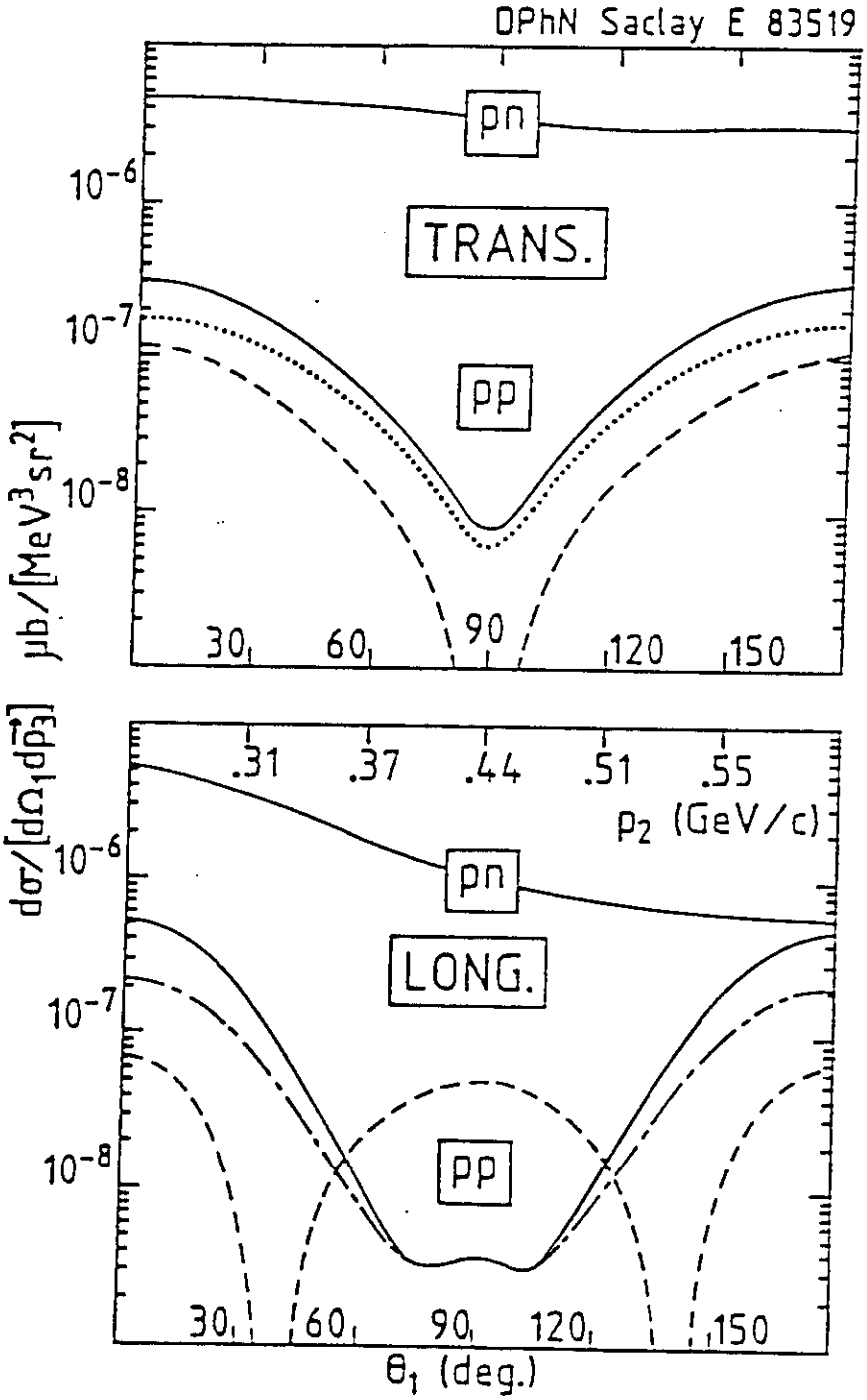

Figure 27 Angular distributions of the reduced cross sections for the ^{3}He(e,e'2p)n reaction at e = 570 MeV, ω = 200 MeV, $\theta = 25°$. (– – –) PW without MEC, (.....) PW with MEC, (–.–.–) including pp rescattering, (——) including all FSI (from ref. 38)

VI. Free and Bound Nucleon Electromagnetic Responses

a) Free Nucleon Form Factors

As mentioned already, a major part of the physics programs at the new electron facilities will concern systematic studies of the few nucleon systems. Key ingredients for such studies are the form factors for the free nucleon themselves, and a detailed understanding of how the electron-nucleon interaction is possible modified in medium. For free nucleons G_E^n, the neutron electric form factor, is the most poorly known. The available body of data up to $Q^2 \sim 1.5$ (GeV/c)^2 are shown in figure 29 (from ref. 40). At high Q^2, models in which the vector dominance hypothesis is merged into a perturbative QCD regime[30] suggest $F_{1n} \simeq 0$, i.e. $G_E^n \sim G_M^n$ at 4 (GeV/c)^2. Possible reactions which can be exploited to measure G_E^n are

(a) $^2\vec{H}(\vec{e}, e'n)$ p
(b) $^2\vec{H}(\vec{e}, e')$ x
(c) $^2H(\vec{e}, e'\vec{n})$p
(d) $^3\vec{H}_e(\vec{e}, e')$x

An experiment to measure G_E^n using reaction (c) is underway at Bates. We describe briefly two experiments proposed for CEBAF[41] exploiting reactions (d) and (a).

The first method(d) consist in measuring the beam asymmetry

$$A = \frac{\sigma(+) - \sigma(-)}{\sigma(+) + \sigma(-)} \tag{13}$$

for longitudinally polarized electrons scattered off a polarized ^{3} He target, at the top of the quasielastic peak. It has been shown[42] that 90% of this asymmetry is due to the neutron

$$A_{e_{H_e}} \approx A_{en} \cdot \frac{\sigma_n}{\sigma_n + 2\sigma_p} \text{ with } A_{en} = \frac{aG_M^{n^2}\cos\theta^* + bG_M^n G_E^n \sin\theta^*\cos\phi^*}{cG_M^{n^2} + dG_E^{n^2}} \tag{14}$$

For a given Q^2, A = 0 at θ_o^* such that

$$R = G_E^n/G_M^n = -a\cot\theta_o^*/b\cos\phi^* \tag{15}$$

so the determination of θ_o^* gives G_E^n/G_M^n

Counting rates have been estimated assuming 10^{18} atoms/cm^2 of ^{3}He with polarization 50%[43] and a beam of intensity 200 μ A and polarization 40%. Such low luminosities ($\sim 10^{33}$ cm $^{-2}$ sec^{-1}) are compatible with the Large Acceptance Spectrometer ($\sim$ 0.8 x 4π) studied at CEBAF[44]. About 20 days would be necessary for two measurements at $Q^2 = 0.2$ and 1(GeV/C)^2 with $\pm$ 20% accuracy on the ratio G_E^n/G_M^n.

The other method, exploiting reaction (a), would make use of a solid ND_3 target, polarized in the scattering plane perpendicular to the momentun transfer $\vec{q}$. Vector polarization rates of 60% can be achieved at 250°mK in a 5T magnetic field [45]. With a 3 cm (1.6 10^{23} neutrons/cm^2) target, and a beam of intensity 10 nA and polarization 40%,

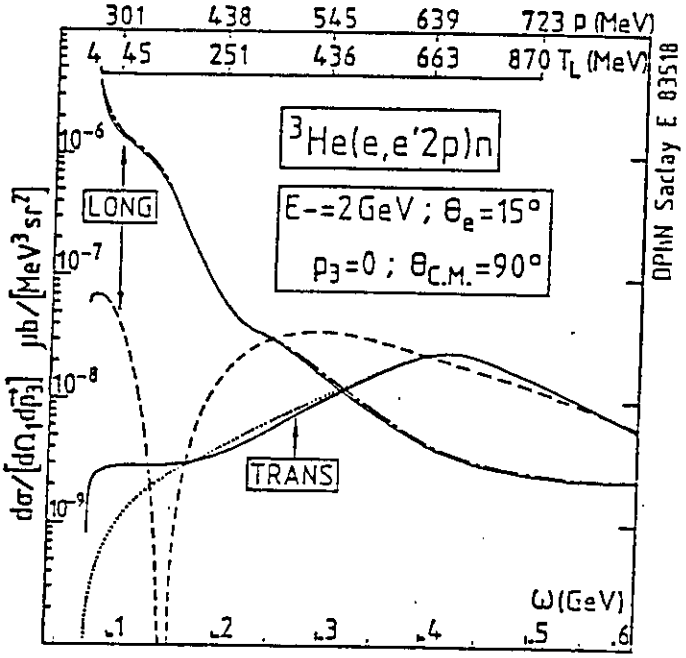

Figure 28 Excitation functions for the ^{3}He(e,e'2p)n reaction at e = 2 GeV, $\theta_e = 15°$. Curves as in fig. 27 (from ref. 38)

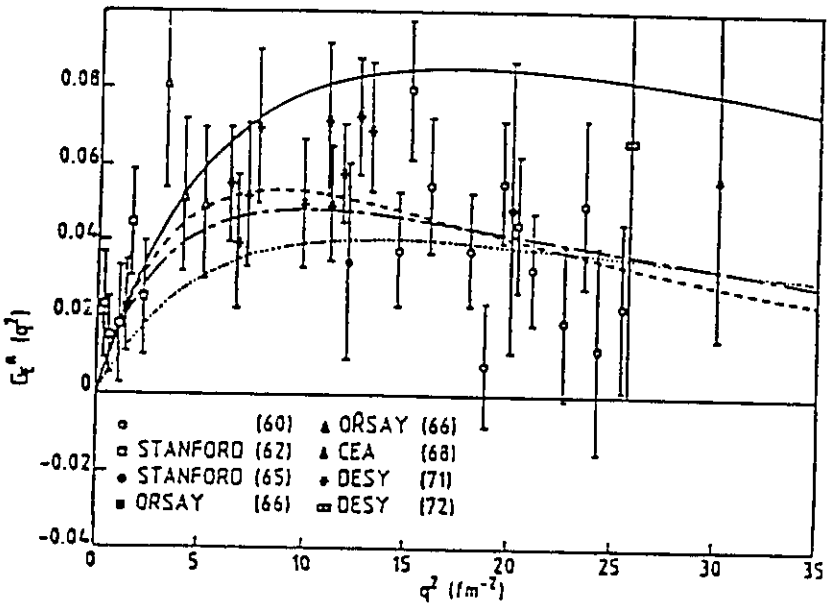

Figure 29 Available data for the neutron electric form factor G_{En}

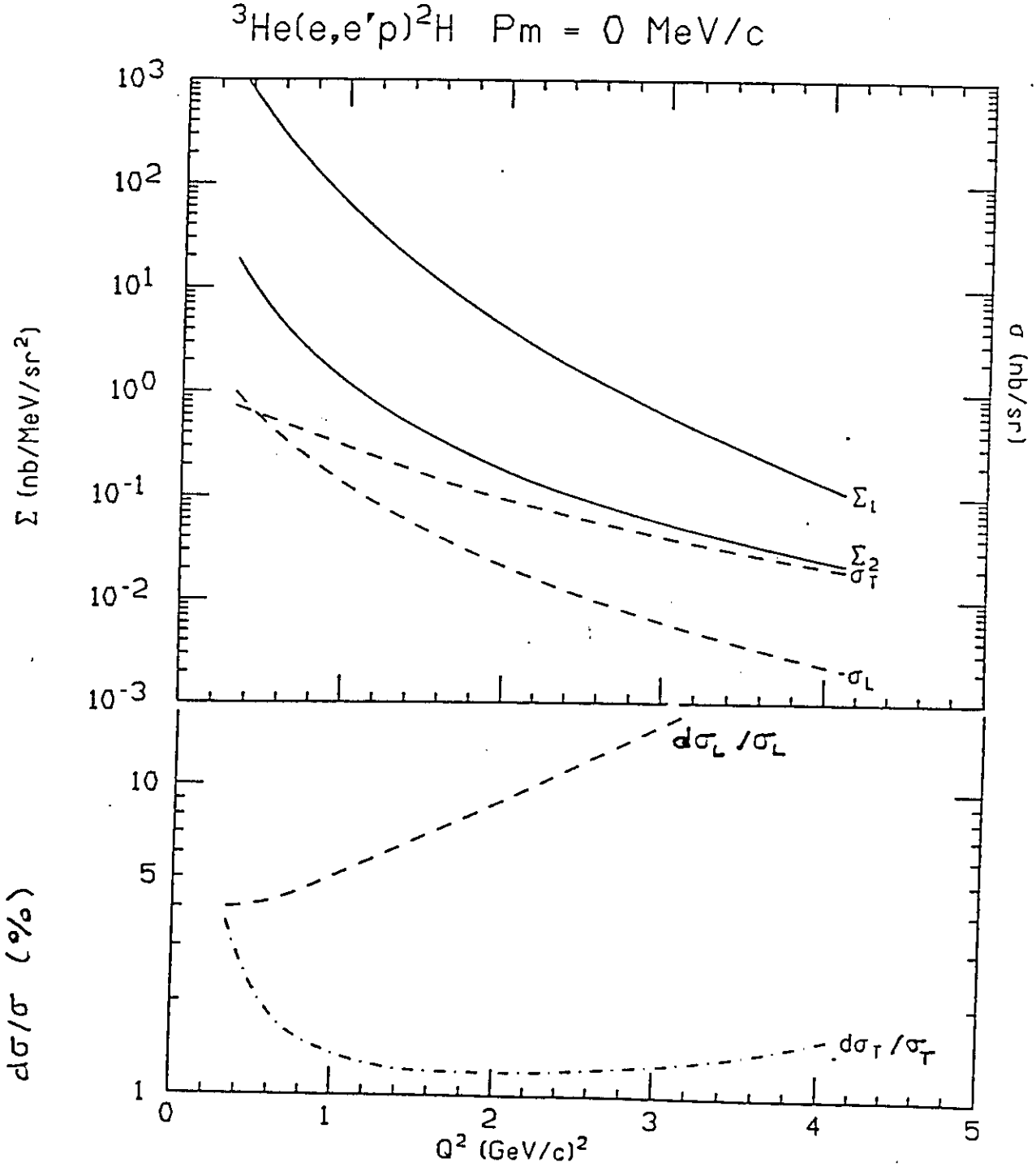

Figure 30 Total differential forward (Σ_1) backward (Σ_2) and reduced (σ_T, σ_L) cross sections for the ^{3}He(e,e'p)d reaction at $p_m = 0$. The lower part of the figure shows relative uncertainties in σ_L/σ_T separations which could be achieved at CEBAF (see text)

assuming 50% neutron detection efficiency within $\Delta\Omega_n = 70$ msr, running times are as follows for $\Delta A/A = \pm 20\%$

Q^2 (GeV/c)^2:	0.5	running time (hrs):	50
	1.		300
	1.5		700

b) Bound Nucleon Responses

Near the top of the quasielastic peak where one-nucleon knock-out processes dominate, the (e,e'N) reaction on nuclei can be used to study the electromagnetic properties of nucleons inside the nuclear medium. The usual description of the quasifree process assumes the validity of the impulse approximation, i.e. the use of free-nucleon currents. However, since the nucleon is an extended object, the nucleon spinor, the nucleon form factors and the current operator are likely be modified in medium. Already, interaction effects shift the nucleon off-mass-shell, and different expressions for the relativistic nucleonic current like

$$\bar{U}(\vec{p}\,') \left[\gamma_\mu F_1 - i\sigma_{\mu\nu}\, \vec{q}^{\,\nu}\, \frac{KF_2}{2M} \right] U(\vec{p}) \tag{16}$$

or

$$\bar{U}(\vec{p}\,') \left[\gamma_\mu (F_1 + KF_2) + (p'_\mu + p_\mu) \frac{KF_2}{2M} \right] U(\vec{p}) \tag{17}$$

which are identical for free nucleons will give different results when extrapolated off-shell[46]. Various prescriptions have been used[47] and, provided that Lorentz and gauge invariance are preserved, the "off-shell ambiguities" are small in most cases, at least near the quasifree peak. This only means that impulse approximation can still be a well defined concept, but do not ensure its validity.

Indeed, relativistic mean field theories imply a modification of nucleon spinors and current operators. In the so-called σ-ω model, the spinors are solutions of a modified Dirac equation

$$(\vec{\gamma}\cdot\vec{p} - M^*)\, U^*(\vec{p}) = \gamma^o E^*\, U^*(\vec{p}) \tag{18}$$

where $M^* = M + V_s$ and $E^* = E - V_o$ with $V_s \sim -400$ MeV and $V_o \sim 300$ MeV being the potentials associated with the strong σ and ω fields. Using free nucleon form factors, this approach has been reasonably successful in explaining inclusive (e,e') data at the quasifree peak[46,48]

More recently, the possibility for the intrinsic properties of the nucleon to be modified in medium has been raised, mainly from deep-inelastic studies at high momentum transfer[49]. This problem is under active investigation through various approaches. One is the idea that the peripheral structure of the nucleon, i.e. its pion cloud, get modified (enhanced) in the nucleus[50]. This may lead to an increase of the proton mean charge radius $\Delta < R_c^2 >$ of ~ 0.4 fm^2, resulting in a quenching of the electric form factor[51]. Skyrmion models relate the nucleon mass and radius to the coupling constants g_A and f_π, which are modified in medium

$$R(\rho) = C\sqrt{g_A(\rho)}\,/\,f_\pi(\rho) \qquad M_N^*/M_N = f_\pi(\rho)/f_\pi. \tag{19}$$

From a study of axial currents in nuclei, Rho[52] obtains in nuclear matter $M_N^*/M_N = 0.62$ and $R(\rho)/R_o = 1.44$.

The idea of an increase of the confinement radius due to an increase in correlation length between quarks (dynamical rescaling) has been proposed [53]. Typically $R_A^C/R_N^C \sim 1.15$ for ^{56}Fe. Soliton models[54] predict also a density dependence of the nucleon electromagnetic radius and magnetic moment.

As mentioned in section II, the present data do not allow to draw definite conclusions on this subject. With the advent of high energy continuous electron beams like CEBAF, systematic studies of the Q^2-dependence of the quasifree (e,e'p) cross section, with longitudinal/transverse separations, can be performed to investigate these effects. As pointed out by DeWitt-Huberts[55], by selecting discrete states of well defined angular momentum probing different regions of the nucleus, one can study the density-dependence of the photon-nucleon coupling in the medium. Counting rates have been estimated under CEBAF conditions for the ^{3}He(e,e'p)^{2}H reaction taken as an example[36]. Under the following kinematical constraints

$$E_e \leq 4GeV \qquad E_{e'} \geq 0.4GeV \qquad p' \leq 3GeV/c$$
$$\theta_e \geq 10^o \qquad \theta_p \geq 10^o$$

and assuming systematic errors to be controlled to 1%, it seems possible (figure 30) to separate the longitudinal and transverse cross sections up to $Q^2 \sim 3.2$ $(GeV/c)^2$, with $\Delta\sigma_L/\sigma_L \sim 20\%$ at the highest Q^2 value, in a reasonable amount of running time. For example, with 5.10^{35} $cm^{-2}sec^{-1}$ luminosity and the CEBAF Hall A spectrometers, counting rates of 4200 (490) events.hr^{-1} for the forward (backward) angle measurement can be obtained, accidental coincidence rates being negligible.

Conclusion

I tried to show from a few examples that the study of nuclei via the (e,e'N) reaction is a very rich and promising field, especially in view of the new continuous beam electron facilities under construction or in project. Although the analysis of data is complex because many features of the hadronic system are involved, exclusive (e,e'N) and (e,e'2N) reactions are relatively simple channels for which quantitative interpretations can be undertaken. The need to go beyond the naive quasifree knock-out picture is already evident from the most recent coincidence experiments. Separation of the various structure functions, study of Q^2-dependence, measurement of polarization observables and broad systematic studies over a wide variety of kinematical and dynamical constraints seem to be the most promising approaches.

References

(1) C. Marchand et al, Phys. Lett. 153B, 29 (1985)
(2) H.J. Pirner et al., Phys. Rev. Lett. 46, 1376 (1981)
(3) G.E. Brown et al., Phys. Lett. 118B, 39 (1982)
(4) R. Altemus et al., Phys. Rev. lett. 44, 965 (1980)
(5) P. Barreau et al., Nucl. Phys. A402, 515 (1983)
(6) Z.E. Meziani et al., Phys. Rev. lett. A52, 2130 (1984)
(7) M. Deady et al., Phys. Rev. C33, 1987 (1986)
(8) C.C. Blatchley et al., Phys. Rev. C34, (1986)
(9) Z.E. Meziani, Few-body Systems Suppl. 1, 354 (1987)
(10) Y. Horikawa et al., Phys. ref. C22, 1680 (1980)
(11) J. M. Laget, Lect. Notes Phys 137, 148 (1981)
(12) P.J. Mulders, Nucl. Phys. A459, 525 (1986)
(13) S. Frullani and J. Mougey, Adv. Nucl. Phys. 14, 1 (1984)
(14) D.S. Koltun, Phys. Rev. lett. 43, 1143 (1972)
(15) J. Morgestern, Proc. of the Fourth Miniconference, NIKHEF-K (1985), p. 52 and C. Marchand et al., to be published.
(16) J.M. Laget Phys. Lett. 51B, 325 (1985)
(17) R.W. Lourie et al, Phys. Rev. Lett. 56, 2364 (1986)
(18) H. Baghaei et al., MIT PhD Thesis (1987) and to be published
(19) S. Homma et al., Phys-Rev. C27., 31 (1983)
(20) G. van der Steenhoven, Phys. Rev. Lett. 57, 1982 (1986)
(21) J. Morgenstern, Nucl. Phys. A446, 315c (1985) and D. Reffay-Pikeroen, to be published.
(22) W. Fabian and H. Arenhövel, Nucl. Phys. A314, 253 (1979)
(23) T. W. Donnelly, Prog. Part. Nucl. Phys. 13, 183 (1984)
(24) S. Boffi et al., Nucl. Phys. A435, 697 (1985)
(25) A. Picklesimer et al., Phys. Rev. C32, 1312 (1985)
(26) S. Boffi et al., Proc. 1986 CEBAF Summer Workshop, p. 133
(27) R. Arnold et al. , Phys. Rev. C21, 1426 (1980)
(28) P. Bosted, Proc. 1987 CEBAF Summer Workshop, p. 143 554
(29) W. Turchinetz, Few Body Systems, Suppl. 1 (1987), p. 326
(30) M. Gari and W. Krümpelmann, Z. Phys. A322, 689 (1986)
(31) F. Coester and W.M. Polyzou, Phys. Rev. D6, 1348(1982)
P.L. Chung et al., in preparation.
(32) W. Polyzou, private communication, May 1987
(33) Ch. Hadjuk et al., Nucl. Phys. A405, 581 (1983)
H. Meier-Hadjuk et al., Nucl. Phys. A395, 332 (1983)
J. L. Friar, Few Body Systems, Suppl. 1, (1987) p. 94
(34) C. Ciofi degli Atti et al., Phys. Lett. 141B, 14 (1984)
R. Schiavilla et al., Nucl. Phys. A449, 219 (1986)
(35) E. van Meijgaard and J. A. Tjon, Few Body Systems Suppl. 1, 307 (1987)

(36) J. Mougey et al., Report to the CEBAF Program Advisory Committee, Feb. 1987, unpublished.
(37) P. H. M. Keizer et al., Phys. Lett. 157B, 255 (1985)
(38) J. M. Laget, Phys. Rev C35, 832 (1987)
(39) J. Lightbody et al., Report to the CEBAF Program Advisory Committee, Feb. 1987, unpublished
(40) S. Kowalski, Nucl. Phys. A446, 363c (1985)
(41) J. McCarthy et al., Report to the CEBAF Program Advisory Committee, Feb. 1987, unpublished
(42) B. Blankleider and R.M. Woloshyn, Phys. Rev. C29, 538 (1984)
(43) R. G. Milner et al., Contr. to 1986 CEBAF Summer Study group, p. 685
(44) B. Mecking, Proc. 1987 CEBAF Summer Workshop, p. 383
(45) V. Burkert, Contr. to 1985 CEBAF Summer Study Group, p. 9-1
(46) T. De Forest, Phys. Rev. Lett. 53, 895 (1984)
(47) T. De Forest, Nucl. Phys. A392, 232 (1983); see also ref. 13.
(48) J. V. Noble, Phys. Rev. Lett. 46, 412 (1981)
(49) R. G. Arnold et al, Phys. Rev. Lett. 52, 727 (1984)
(50) C. H. Llewellyn - Smith, Phys. Lett. 128B, 107
(1983) M. Ericson and A.W. Thomas, Phys. Lett. 128b, 112 (1983)
(51) M. Ericson and M. Rosa.Clot, CERN-TN 4420 (1986)
(52) M. Rho, Phys. Rev. Lett. 54, 767 (1985)
(53) R. L. Jaffe, Phys. Rev. Lett. 50, 228 (1983)
F.E. Close et al., Phys. Lett. 129B, 346 (1983)
(54) M. Jändel and G. Peters, Phys. Rev. D30, 1117 (1984)
L. S. Celenza et al., PR C12, 212, 232 (1985)
G. Chanfray et al., Phys. Lett. 147B, 249 (1984)
(55) P.K.A. DeWitt Huberts, Proc. Int. Nuclear Physics Conf., Harrogate, U.K., August 1986, J.L. Durell et al., editors, Bristol (1987), p.61.
(56) E. Quint et al., Phys. Rev. Lett. 57, 186 (1986)
(57) N.H. Kwong and J. Hüfner, Phys. Lett. 146B, 370 (1984)